REPORT DOCUMENTATION PAGE			Form Approved OMB No. 0704-0188

OSP 66939

Public reporting burden for this collection of information is estimated to average 1 hour per response, including the time for reviewing instructions, searching existing data sources, gathering and maintaining the data needed, and completing and reviewing the collection of information. Send comments regarding this burden estimate or any other aspect of this collection of information, including suggestions for reducing this burden, to Washington Headquarters Services, Directorate for Information Operations and Reports, 1215 Jefferson Davis Highway, Suite 1204, Arlington, VA 22202-4302, and to the Office of Management and Budget, Paperwork Reduction Project (0704-0188), Washington, DC 20503.

1. AGENCY USE ONLY (Leave blank)	2. REPORT DATE 12/31/01	3. REPORT TYPE AND DATES COVERED Final 12/1/97 – 11/30/2000

4. TITLE AND SUBTITLE	5. FUNDING NUMBERS
Femtosecond Photonics: Fundamental Phenomena and Advanced Devices	F49620-98-1-0139

6. AUTHOR(S)

Profs. Erich Ippen, James Fujimoto, and H.A. Haus

7. PERFORMING ORGANIZATION NAME(S) AND ADDRESS(ES)	8. PERFORMING ORGANIZATION REPORT NUMBER
Research Laboratory of Electronics Massachusetts Institute of Technology 77 Massachusetts Avenue Cambridge, MA 02139	

9. SPONSORING/MONITORING AGENCY NAME(S) AND ADDRESS(ES)	10. SPONSORING/MONITORING AGENCY REPORT NUMBER
Air Force Office of Scientific Research 110 Duncan Avenue, Suite B115 Bolling Air Force Base, DC 20332-8080	2301/AS

11. SUPPLEMENTARY NOTES

The view, opinions and/or findings contained in this report are those of the author(s) and should not be construed as an official Department of the Army position, policy, or decision, unless so designated by other documentation.

12a. DISTRIBUTION/AVAILABILITY STATEMENT	12b. DISTRIBUTION CODE
Approved for public release; distribution unlimited.	

13. ABSTRACT (Maximum 200 words)

During the period of this program we made significant progress in several areas, in the development of new femtosecond lasers and techniques, in the application of ultrafast optics to fiber devices and to studies of novel materials and material structures. Some of these key advances are summarized in sections entitled:

20020107 222

14. SUBJECT TERMS			15. NUMBER OF PAGES
			16. PRICE CODE

17. SECURITY CLASSIFICATION OF REPORT	18. SECURITY CLASSIFICATION OF THIS PAGE	19. SECURITY CLASSIFICATION OF ABSTRACT	20. LIMITATION OF ABSTRACT
UNCLASSIFIED	UNCLASSIFIED	UNCLASSIFIED	UL

NSN 7540-01-280-5500

Standard Form 298 (Rev. 2-89)
Prescribed by ANSI Std. Z39-18
298-102

FINAL REPORT

FEMTOSECOND PHOTONICS:

FUNDAMENTAL PHENOMENA AND ADVANCED DEVICES

Period: December 1, 1997 - November 30, 2000

Principal Investigators

Professor Erich P. Ippen
Professor Hermann A. Haus
Professor James G. Fujimoto

Address

The Research Laboratory of Electronics
Massachusetts Institute of Technology
77 Massachusetts Avenue
Cambridge, MA 02139

1

FINAL REPORT

Period: December 1, 1997 - November 30, 2000

Air Force Office of Scientific Research   Contract No. F49620-98-1-0139

Principal Investigators

> Professor Erich P. Ippen
> Professor Hermann A. Haus
> Professor James G. Fujimoto

Other Personnel Supported

Dr. Yijang Chen, Dr. Franz Kärtner, Dr. Uwe Morgner, Dr. Patrick Langlois, Dr. Marcus Joschko, Dr. Kaoru Minoshima, Igor Bilinsky, Seong-Ho Cho, Matthew Grein, Boris Golubovic, David Jones, Rohit Prasankumar, Erik Thoen, William Wong and Charles X. Yu

Objectives

To investigate fundamental femtosecond-timescale phenomena in photonic materials and device structures. To evaluate the potential of these phenomena for device applications. To invent and demonstrate new devices for ultrafast optics.

Status and Accomplishments

During the period of this program we made significant progress in several areas, in the development of new femtosecond lasers and techniques, in the application of ultrafast optics to fiber devices and to studies of novel materials and material structures. Some of these key advances are summarized in sections entitled:

1. Ultrashort pulse femtosecond lasers
2. Optical phase and waveform control of sub-two-cycle pulses
3. Dispersion managed propagation and modelocking
4. Noise in ultrafast optical devices
5. Generation of high intensity ultrashort pulses using novel laser design
6. Nonlinear semiconductor mirrors for femtosecond pulse generation
7. Erbium glass waveguide lasers and short pulse generation
8. Nonepitaxial saturable absorber materials for nonlinear optic
9. Ultrashort pulse fiber lasers
10. Photonic device fabrication using nonlinear materials processing

A list of publications acknowledging this contract is appended at the end.

1. Ultrashort pulse femtosecond laser technology

Ultrashort pulse femtosecond lasers and ultrafast technology have widespread applications in such diverse areas as basic research in physics, chemistry, and biology as well as high speed telecommunications, photonics and biomedicine. Pulse duration, center wavelength, output-power, as well as complexity and cost are important parameters for most applications. During the last three years, we developed new ultrashort laser technology based on the use of DCMs for dispersion compensation. Chirped and double-chirped mirrors can control the dispersion inside a laser cavity more accurately than standard prism compressor configurations. In chirped mirrors, the variation of the Bragg wavelength during the layer growth leads to a deeper penetration of longer wavelengths [2]. This variation results in a broad reflectivity range and a negative dispersion of the reflected pulse. However, the wavelength dependent negative dispersion is superimposed by strong oscillations. The dispersion oscillations arise because long wavelengths are reflected weekly from the front sections of the mirrors on their way deep inside the mirror. The interference of the weakly reflected light from the mirror front section with light strongly reflected deep inside the mirror causes group delay oscillations similar to a Gires-Tournois interferometer. In DCMs, the coupling coefficient of the Bragg mirror is also chirped by gradually increasing the thickness of the high index layer. In this way, the oscillatory behavior can be reduced and the bandwidth of the mirrors can be increased significantly [3]. As the phase characteristics of the DCMs are extremely sensitive to variations in the layer thickness our DCMs were grown by ion-beam sputtering, the state-of-the-art technique for dielectric multi-layer depositing of DCMs [4]. Our application of novel DCMs to $Ti:Al_2O_3$ and Cr:forsterite resulted in the generation of the shortest pulses and broadest bandwidths ever produced from these laser materials at 0.8 µm and 1.3 µm center wavelength, respectively [5, 6].

Ti:sapphire laser using DCMs: We developed a Kerr-lens mode-locked Ti:sapphire laser that produces pulses shorter than 5.4 fs at 800 nm center wavelength. The corresponding spectral bandwidth is greater than 350 nm at 90 MHz repetition rate and 200 mW average output power. This world-record pulse duration is based on newly designed and fabricated DCMs for dispersion compensation. D. Sutter *et. al.* have also generated sub-two cycle pulses from a Ti:sapphire laser[7]. Our Ti:sapphire laser uses a standard z-fold cavity-design, as shown in Fig. 1.1. The Ti:sapphire crystal (thickness 2.05-mm) is placed between two curved mirrors with 100 mm radius of curvature. All mirrors in the cavity are DCMs, except the output-coupling mirror (OC) and silver mirror (M_0). The DCMs accounted for the dispersion of the laser rod. Two Brewster-cut CaF_2-prisms are used for minor adjustments to the dispersion compensation. Each prism is mounted on a translation stage. Therefore, the prism insertion into the laser beam can be controlled. In addition, mounting the prism P_1 and the end-mirror M_0 on a translation stage permits the continuous variation of the prism separation. Slightly moving the translation stage with P_1 starts Kerr-lens mode-locking.
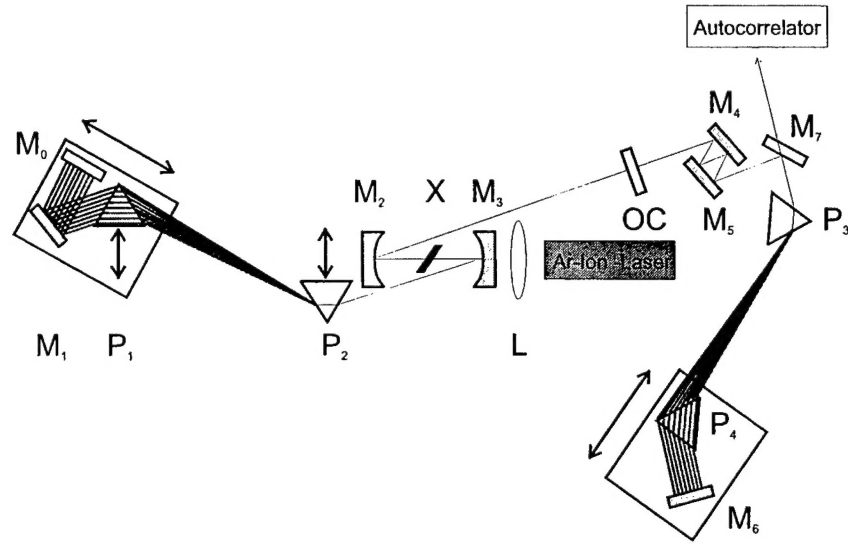
Figure 1.1: Schematic of Ti:sapphire laser: The double chirped mirrors (DCM) M_1-M_3 in combination with the CaF$_2$ prisms P_1 and P_2 compensate the dispersion of the Ti:sapphire crystal X (l=2.5 mm) and the output coupling mirror OC inside the cavity. The DCMs M_4-M_6 in combination with the fused silica prisms P_3 and P_4 compensate the dispersion outside the laser cavity. M_0 and M_7 are silver mirrors.

After passing the 1.5% OC, the beam reflects four times from the DCMs (M_4, M_5) and passes through a pair of fused-quartz prism (P_3, P_4) outside the cavity. Again, the prism insertion and separation can be controlled independently. In this way, a certain amount of third order dispersion can be compensated for. The prism pair can also compensate for the dispersion in the autocorrelator, which is a standard interferometric design with two counter-oriented metallic beam splitters on a 0.1-mm substrate and a 30-µm thin KDP crystal.
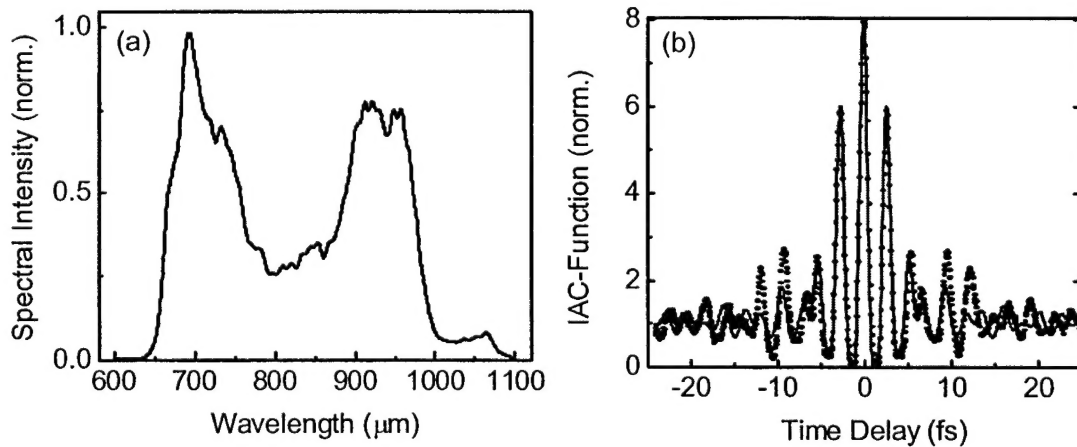

Figure 1.2: (a) Spectrum of the Ti:sapphire laser extending from 650-1000 nm. (b) Interferometric autocorrelation measurement (dots). The solid line represents a sinc^2-fit assuming with a FWHM of 5.4 fs.

The spectrum of the laser pulses is shown in Fig. 1.2(a). The bandwidth is greater than 350 nm, covering the range from 0.65 to 1 µm. An interferometric autocorrelation of the

ultrashort pulses is shown in Fig. 1.2(b) (dots). The intracavity prism separation was 65 cm, and the insertion of P_2 ~2 mm and P_1 ~5 mm. A fit of a sech-shaped pulse would result in a pulse width of 4.3 fs FWHM, while a fit to Gaussian-shaped pulse results in 4.8 fs. The most conservative assumption of a sinc-shaped pulse gives a pulse duration of 5.4 fs (solid line). The good agreement of the measured autocorrelation with the autocorrelation function derived from the spectrum indicate a pulse width between 4.9-5.4 fs, which corresponds to less than two optical cycles at the center wavelength of 800 nm. The Ti:sapphire laser has already been applied to ultrahigh resolution OCT imaging studies *in vivo* in developmental biology specimens [8] and human retina [9].

To date, the pulse duration is limited by the bandwidth over which the DCMs can balance the dispersion inside the cavity. The gain bandwidth of Ti:sapphire, extending from 0.6-1.2 µm, would enable shorter pulses in the single-cycle regime. However, increasing the bandwidth of the DCMs would result in stronger oscillations of the group delay, which limits the pulse duration. Since the phase of the group delay oscillations depends on the index of refraction of the dielectric layers and the layer thickness, the phase can be controlled. Therefore, two sets of ultra-broadband DCMs can be designed with oscillations that are exactly out of phase. In these two mirror sets the oscillations would add up to zero. This approach would allow for dispersion compensation over an increased spectral range resulting in broader bandwidth and shorter pulse durations. This novel approach might enable the generation of single-cycle pulses.

Cr:forsterite laser using DCMs: An all-solid-state, Kerr-lens mode-locked Cr:forsterite laser producing 14-fs pulses with 250 nm bandwidth at 1.3 µm was built using DCMs for dispersion management inside the laser cavity. An average power of 80 mW at 100 MHz repetition rate was achieved. These pulses represent the shortest pulses ever produced by a Cr:forsterite laser [6, 10]. The spectral range at 1.3 µm is of particular interest because it falls into the 2nd telecommunication window. In addition, the zero dispersion wavelength of most materials falls into this wavelength range. Since Cr:forsterite is a low gain laser material, maximum reflectivity of the mirrors is important. The reflectivity of our DCMs remains greater than 0.998 from 1.1-1.5 µm, resulting in a bandwidth of 400 nm. At shorter wavelengths of <1.10 µm, the reflectivity decreases rapidly for high transmission of the pump beam at 1.064 µm.

In the 1.3 µm wavelength range, dispersion compensation is particularly challenging because higher order dispersion becomes the dominant factor near the zero dispersion wavelength. Higher order dispersion is hard to compensate over an extended wavelength range with DCMs. Therefore, it is important to minimize higher order dispersion in the cavity by reducing the crystal length and choosing the optimum prism material. We have chosen PBH71 (SF58) as prism material with a zero dispersion wavelength of 2 µm. This zero dispersion wavelength at much longer wavelengths than the lasing wavelength results in a favorable ratio of second to third order dispersion in the lasing range and enables broadband DCMs. The DCMs were fabricated by ion-beam sputtering, the state-of-the-art technique for dielectric multi-layer depositing [4]. All mirrors in the cavity are DCMs except for the output-coupling mirror. This setup results in 5 bounces on DCMs

per round-trip. Two Brewster-cut, high dispersion PBH71-prisms are used for adjusting the dispersion compensation. The insertion of each prism into the laser beam and the prism separation can be controlled by translation stages permitting the compensation of second and third order dispersion. The dispersion contribution of the laser rod, the prism material and the DCM inside the laser cavity are shown in Fig. 1.3. The DCMs in combination with the PBH71 prisms balance the dispersion in the range from 1.2-1.48 μm. This dispersion compensation results in the broad spectrum with 250-nm bandwidth (FWHM) shown in Fig. 1.4(a) and enables the generation of 14-fs pulses as shown by the interferometric autocorrelation in Fig. 1.4(b). These pulses are the shortest pulses ever produced directly from a Cr:forsterite laser.
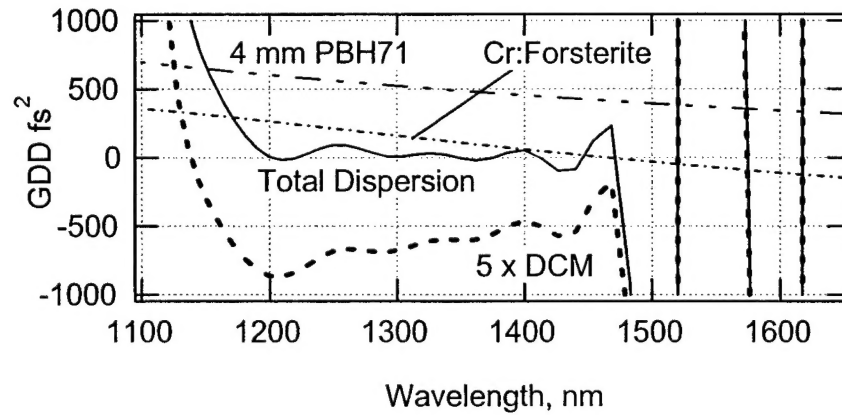

Figure 1.3: Dispersion management of the Cr:forsterite laser. The dispersion introduced per roundtrip is shown for all the material present the cavity. The DCMs in combination with the PBH71 prisms balance the dipersion over 300 nm, from below 1200 nm to almost 1500 nm (solid line).
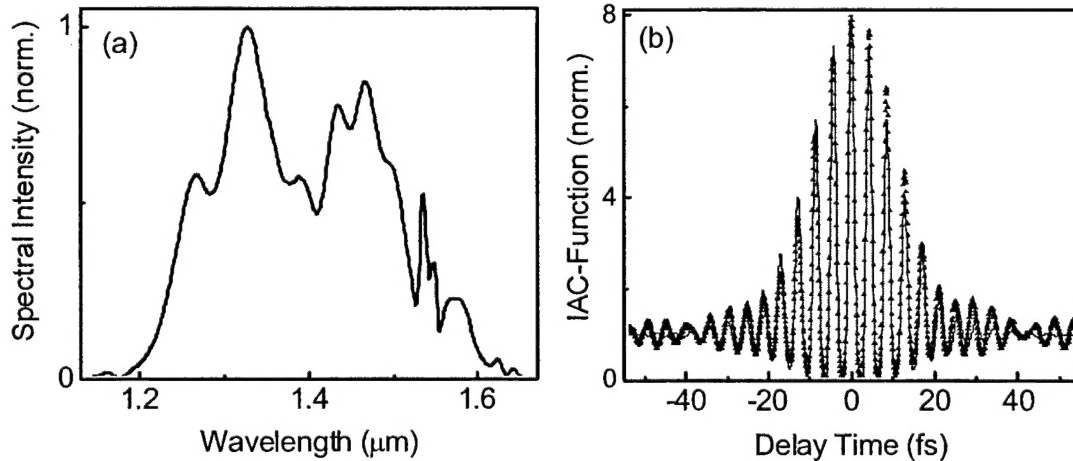

Figure 1.4: (a) Output spectrum of the Cr:forsterite laser showing 250 nm FWHM bandwidth. (b) Interferometric autocorrelation measurement (triangles). The solid line represents a sech-fit assuming 14 fs pulse duration.

<u>Diode pumped Cr:forsterite laser:</u> We have also successfully developed a Cr:forsterite laser producing world record pulse durations. With further advances, we believe that the performance of this laser can be enhanced still further. To date, the spectral bandwidth

and hence the pulse duration of the laser is limited by the spectral bandwidth over which the DCMs balance the dispersion. The current DCMs, in combination with the PBH71 prisms, balance the dispersion in the range from 1.2-1.48 µm (see Fig.3). At lower wavelengths, the need for high transmission at 1.064 µm for high pump efficiency limits the dispersion management. Therefore, we propose to develop a direct diode pumped Cr:forsterite laser. Because the pump wavelength is shifted 85 nm to a lower wavelength at 980 nm, we can design new DCMs that balance the dispersion over an extended spectral range. These new DCMs may enable the generation of spectral bandwidths exceeding 330 nm. Such laser pulses would have pulse durations below 10 fs, reaching the 1-2 optical cycle regime. In OCT imaging these pulses would enable an image resolution of about 3 µm in air and about 2 µm in tissue. This laser would also be a powerful tool for studies of ultrafast phenomena in materials and devices. Finally, a diode pumped solid state laser could be engineered into a compact and lower cost system, enabling commercial applications.

References for Section 1

1. Y. Chen, F.X. Kartner, U. Morgner, S.H. Cho, H.A. Haus, E.P. Ippen, and J.G. Fujimoto, "Dispersion-managed mode locking," Journal of the Optical Society of America B Optical Physics, 1999. 16(11): p. 1999-2004.
2. A. Stingl, C. Spielmann, F. Krausz, and R. Szipocs, "Generation of 11-fs pulses from a Ti:sapphire laser without the use of prisms," Optics Letters, 1994. 19(3): p. 204-6.
3. F.X. Kärtner, N. Matuschek, T. Schibli, U. Keller, H.A. Haus, C. Heine, R. Morf, V. Scheuer, M. Tilsch, and T. Tschudi, "Design and fabrication of double-chirped mirrors," Optics Letters, 1997. 22(11): p. 831-33.
4. M. Tilsch, V. Scheurer, J. Staub, and T. Tschudi, in SPIE. 1994: SPIE.
5. U. Morgner, F.X. Kaertner, S.H. Cho, Y. Chen, H.A. Haus, J.G. Fujimoto, E.P. Ippen, V. Scheuer, G. Angelow, and T. Tschudi, "Sub-two-cycle pulses from a Kerr-lens mode-locked Ti:sapphire laser," Optics Letters, 1999. 24(6): p. 411-13.
6. C. Chudoba, J.G. Fujimoto, E.P. Ippen, H.A. Haus, U. Morgner, F.X. Kärtner, V. Scheurer, G. Angelow, and T. Tschudi, "All-solid-state Cr:forsterite laser generating 14-fs pulses at 1.3 µm," (Postdeadline), in Conference on Lasers and Electro-Optics (CLEO). 2000. San Francisco (USA): Optical Society of America.
7. Y.P. Tong, P.M.W. French, J.R. Taylor, and J.O. Fujimoto, "All-solid-state femtosecond sources in the near infrared," Optics Communications, 1997. 136: p. 3-4.
8. W. Drexler, U. Morgner, F.X. Kaertner, C. Pitris, S.A. Boppart, X.D. Li, E.P. Ippen, and J.G. Fujimoto, "In vivo ultrahigh resolution optical coherence tomography," Optics Letters, 1999. 24: p. 1221-1223.
9. W. Drexler, U. Morgner, R.K. Ghanta, F.X. Kaertner, J.S. Schuman, and J.G. Fujimoto, "Ultrahigh resolution ophthalmic optical coherence tomography," Nature Medicine, 2000. in press.
10. C. Chudoba, J.G. Fujimoto, E.P. Ippen, H.A. Haus, U. Morgner, F.X. Kärtner, V. Scheurer, G. Angelow, and T. Tschudi, "All-solid-state Cr:forsterite laser generating 14-fs pulses at 1.3 µm," Opt. Lett., 2000.

2. Optical phase and waveform control of sub-two-cycle pulses

We have recently demonstrated for the first time the generation of pulses shorter than two optical cycles directly from a laser oscillator.[1] The Ti:sapphire laser oscillator, the double-chirped mirrors (DCM's) and the realization of dispersion-managed modelocking that made this possible are discussed in sections 2 and 4. One of the implications of such short pulses is the enormous breadth of spectrum that accompanies them. This spectral width of 350 nm that we have achieved creates new opportunities for low coherence based technologies such as optical coherence tomography (OCT), where these broad bandwidths can enable submicron depth resolution. A second implication, the subject of this section, is that it becomes possible to consider determining and controlling the absolute optical phase of the electric field with respect to the envelope of the pulse. This is an important goal of our research. Control of the optical phase will make it possible to create optical frequency standards that are direct multiples of the radio frequency repetition rate of the femtosecond laser. It will also make it possible for the first time to investigate nonlinear optical and physical phenomena that are sensitive to the precise form of the electric and magnetic field waveforms.

A freely propagating pulse consisting of many optical cycles may, to good approximation be described by an amplitude envelope function that does not depend upon the phase of the optical wave it modulates. When the pulse propagates in a medium in which the group velocity differs from the phase velocity, the optical phase slides relative to the envelope, which is relatively unaffected by this sliding. If the pulse contains only a few optical cycles, this is no longer true. In order to gain some appreciation for the sensitivity of ultrashort pulses to the optical phase, consider a simple comparison. If we assume that there can be no zero frequency component in a freely propagating wave, then $A(t)\sin\omega t$ always has an acceptable spectrum, but $A(t)\cos\omega t$ may not. This implies that as $A(t)\sin\omega t$ propagates in a dispersive medium it cannot simply accumulate a frequency independent optical phase shift. Otherwise the spectrum would change, especially at low frequencies. Instead, it distorts and the zero crossings of the field as a function of time become nonuniformly spaced. The spectrum of a pulse does not change under such conditions, but the temporal field waveform clearly does. Even very sophisticated existing methods for pulse characterization such as frequency-resolved optical gating (FROG) are not sensitive to such changes. Ultrafast processes that respond to the instantaneous field will, however, provide different signatures for these different temporal waveforms. A key goal of our work is the observation and study of such nonlinearities using pulses directly from our femtosecond oscillator. That will make it possible to control the laser itself and lock the absolute phase of the output pulses.

A schematic of the modal spectrum of a femtosecond laser output is shown in Figure 2.1. The frequencies are separated by the roundtrip pulse repetition rate $c/2nL$ (where n is the average group index) as are the modes of the cold cavity. But the absolute frequencies are not necessarily exact multiples of $c/2nL$. If the optical phase under the pulse envelope

is sliding from pulse to pulse by an amount $\Delta\phi$ (because the roundtrip phase delay is not the same as the group delay), then the frequency offset is $d\phi/dt = \Delta\phi/(2nL/c)$.
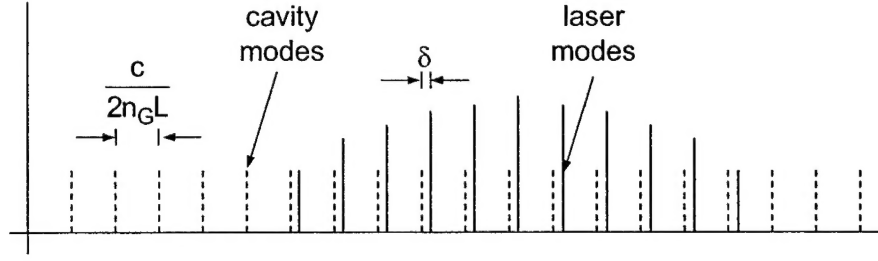

Figure 2.1: The frequencies of a modelocked pulse train (solid lines) and those of the cold cavity (dashed lines). The difference δ is equal to the rate of optical phase slip under the modelocked pulse envelopes caused by different phase and group roundtrip delays.
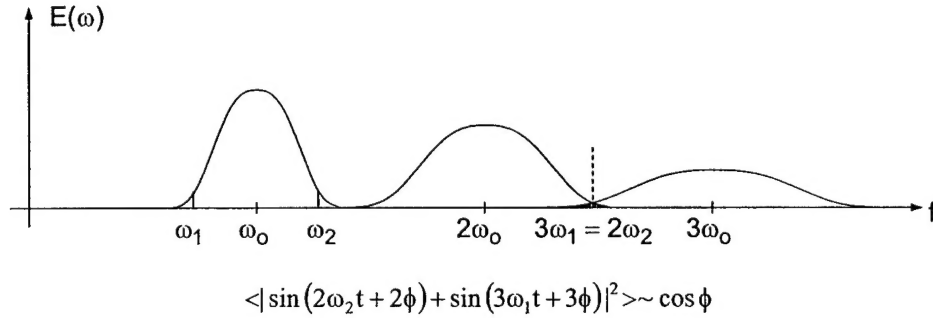

$$< | \sin(2\omega_2 t + 2\phi) + \sin(3\omega_1 t + 3\phi) |^2 > \sim \cos\phi$$

Figure 2.2: Illustration of how the 2nd and 3rd harmonic spectra can interfere. The intensity interference is proportional to $\cos\phi$.

It has recently been shown with spectrally broadened pulse trains that this phase slip can be controlled by frequency doubling a low frequency component and locking it to a fundamental high frequency component (i.e. setting $2mc/2L = pc/2L$ where both m and p are integers) [2,3]. Additional spectral broadening is needed because that scheme requires a full octave of bandwidth. Our scheme for controlling phase is illustrated in Figure 2.2. With only 2/3 of an octave (i.e. with the pulses directly from our oscillator), one can obtain sensitivity to absolute phase by interfering second-harmonic and third-harmonic nonlinear optical signals. The experimental set-up for doing this is shown in Figure 2.3. A very recent, observation of this interference is shown in Figure 2.4, where the rf beats between the c/2L cavity harmonics indicate the rate of phase slip. This is the first optical-phase-dependent nonlinear optical experiment performed with pulses directly from a high repetition rate oscillator.
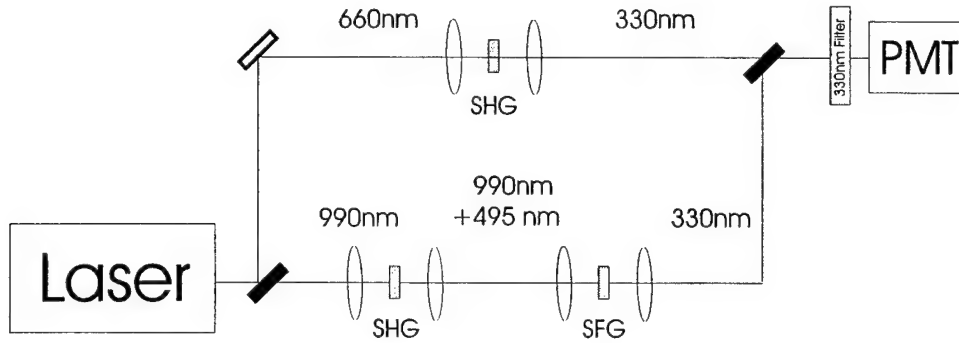
9

Figure 2.3: Set-up for interference of 2nd and 3rd harmonics of the pulse spectrum. Long and short wavelength components are separated at the first beamsplitter to permit maximization of SHG at both ends of the spectrum.
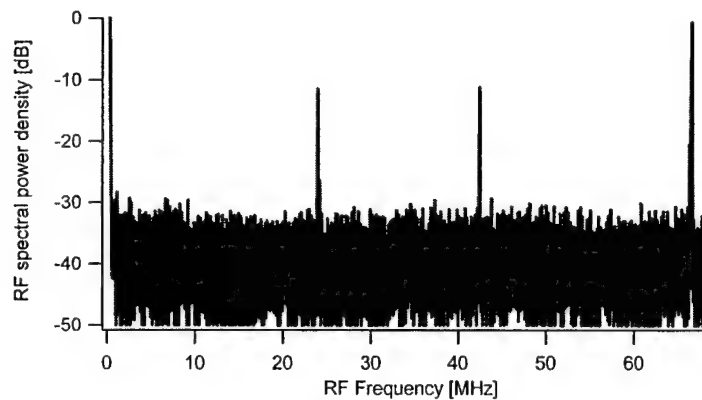

Figure 2.4: The RF spectrum of the 2nd and 3rd harmonic interference. The intense beats are at the pulse repetition frequency and the two in the middle are due to the phase slip.

References for Section 2

1. U. Morgner, F. X. Kaertner, S. H. Cho, Y. Chen, H. A. Haus, J. G. Fujimoto and E. P. Ippen, "Sub-two cycle pulses from a Kerr-lens modelocked Ti:sapphire laser," Opt. Lett. 24, 411 (1999)
2. David J. Jones, Scott Diddams, Jinendra Ranka, Robert Windeler, John L. Hall and Steven Cundiff, "Carrier envelope phase control of femtosecond modelocked lasers and direct optical frequency synthesis," Science, 288, 635 (2000)
3. A. Poppe, A. Apolonskii, G. Tempea, C. Spielman, F. Krausz, T. Udem, R. Holzwarth and T. Haensch, "Controlling the absolute phase of a few-cycle light pulses," CLEO 2000, Postdeadline PD 1, OSA 2000

3. Dispersion managed propagation and modelocking

We have shown that dispersion managed solitons in an ideal (lossless) environment are Nonlinear Bloch Waves [1], that they are self-consistent wave-solutions in a periodically varying self-induced nonlinear potential. In spite of the periodic change of dispersion and

attendant changes of the pulse as it propagates from segment to segment, the pulse is self-shielding; it does not radiate. This should be compared with the case of a standard soliton propagating along a periodically perturbed uniform fiber. This kind of soliton radiates and is gradually depleted by radiation. Perturbations of the ideal periodic structure of the dispersion managed soliton by lumped gain, lumped loss or other perturbations do produce radiation, but much less than in the case of the standard soliton. This fact, which has been observed experimentally, has two causes.

Identical perturbations along different sections of the fiber affect the pulse differently, because the pulse shape is different; their superposition leads to partial cancellation. Dispersion managed solitons operate with much smaller average dispersion than standard solitons. The continuum generated by the perturbation disperses very slowly, because the continuum experiences the average (small) dispersion. Thus, some of the radiation generated by the perturbation can be recaptured by the soliton.

Ultra-short pulse generation has a great deal in common with dispersion managed soliton propagation. In order to generate ultrashort pulses it is necessary to compensate the dispersion of the gain crystal with dispersive mirrors. When a pulse shortens to a few cycles, the dispersion of the gain crystal can stretch the pulse to twice or more of its width. The nonlinearity of the crystal imposes self-phase modulation. The pulse gets recompressed by the dispersive mirrors (and a prism pair for additional fine tuning). Thus the propagation of the pulse is akin to dispersion managed soliton propagation. In the absence of loss and gain and mode-locking action, a pulse can propagate that is akin to a dispersion managed soliton. Hence the dispersion management and the self-phase modulation are fully capable of forming ultra-short pulses. The pulse width is a monotonically decreasing function of pulse energy. The role of the artificial saturable absorber (usually Kerr Lens Mode-Locking) ceases to be that of pulse shaping, but rather as a suppressor of the noise build-up between pulses. This is a very important feature of the system, since the pulse shaping mechanism needs to change the width of an initial pulse by six to seven orders of magnitude, until an ultra-short pulse is achieved. By then the KLM action is highly saturated. If the pulse shaping were left entirely to the KLM action, ultra-short pulses could not be generated. We have recently analyzed the pulse forming action in our two-cycle-pulse laser [2] and find that the experimental observations are consistent with our new theory of dispersion managed modelocking [3].

Dispersion managed long distance soliton propagation is now a concept that has found wide acceptance and is pursued theoretically and experimentally in many research groups. It has not found, as yet, commercial implementation, the main reason being the success of "linear" NRZ (Non-return-to-zero) propagation schemes employing WDM. However, the trend toward higher bit-rates (from 10Gb/s to 40Gb/s) may force the implementation. As the bit-rate increases and with it the bandwidth, a constant signal-to-noise ratio requires higher peak intensities and thus an increase in nonlinear effects. RZ (return-to-zero) formats have found wider and wider commercial applications, in particular since this format gives improved bit-error rates when polarization mode dispersion (PMD) effects are important. Polarization mode dispersion causes separation between two polarizations

of a pulse due to slight difference in group velocities for orthogonal polarizations. Higher bit-rates increase the effect of PMD. The RZ format is akin to the soliton format, and hence soliton propagation occurs naturally. An important recent result of our theoretical work is that we find that solitons may actually self-stabilize against PMD [4]. This is made possible by the nonlinear binding "force" between two orthogonal polarizations of a pulse. This binding force increases with increasing intensity, and thus with increasing bit-rate, so that a soliton is stable for any bit-rate if it is stable at one bit-rate.

References for Section 3

1. H. A. Haus and Y. Chen, "Dispersion-managed solitons as nonlinear Bloch waves," Journal of the Optical Society of America B 16, 889-894, June 1999.
2. U. Morgner, F. X. Kärtner, S. H. Cho, Y. Chen, H. A. Haus, J. G. Fujimoto, E. P. Ippen, V. Scheuer, G. Angelow, and T. Tschudi, "Sub-two-cycle pulses from a Kerr-lens mode-locked Ti:sapphire laser," Optics Letters 24, 411-413, March 1999.
3. Y. Chen, F. X. Kärtner, U. Morgner, S. H. Cho, H. A. Haus, E. P. Ippen, and J. G. Fujimoto, "Dispersion-managed mode locking," Journal of the Optical Society of America B 16, 1999-2004, November 1999.
4. Y. Chen and H. A. Haus, "Solitons and polarization mode dispersion," Optics Letters 25, 290-292, March 2000.

4. Noise in ultrafast optical devices

Ultrafast devices are broadband devices. The sources of quantum noise are white, have a flat spectrum. For this reason, quantum noise tends to be the dominant noise in ultra-fast devices. We have published recently a study of quantum noise in passively mode-locked lasers [1]. If the self-phase modulation is strong, as it tends to be in the case of very short pulses with high peak intensities, the pulse formation mechanism is dominated by self-phase modulation and dispersion (the pulse is soliton-like) as pointed out in Section 3. The pulse has four degrees of freedom, amplitude, phase position and carrier frequency. Quantum mechanically, the pulse behaves both like a particle having position and momentum (i.e. carrier frequency) and a wave, having amplitude and phase. The four degrees of freedom are represented by operators that obey, pair-wise, boson-like commutation relations. Under proper operating conditions, the states of these pairs may approach minimum uncertainty states, the states of lowest noise permitted by quantum mechanics. Experiments on fiber lasers have shown that the timing jitter of the mode-locked pulses is indeed attributable to quantum noise.

Reference for Section 4

1. H. A. Haus, M. Margalit, and C. X. Yu, "Quantum noise of a mode-locked laser," Journal of the Optical Society B 17, 1240-1256, July 2000.

5. Generation of high intensity ultrashort pulses using novel laser design

An important goal in ultrafast optics is to increase laser output pulse energies and intensities. Generation of femtosecond pulses with high intensities in the MW range is essential for a number of applications including nonlinear processes and investigation of ultrafast nonlinear optical phenomena. Since the average output power is constant from a fixed pump power, the pulse energy can be increased by reducing the laser repetition rates in modelocked operation. The reduction of pulse repetition rate from a 100 MHz range to a few MHz represents a significant advantage for nonlinear and ultrafast studies, because it reduces thermal parasitics, sample damage problems, and recovery time artifacts.

Standard femtosecond lasers deliver pulse durations of 50 fs, pulse energies of several nJ, and peak powers of several hundreds of kW. The peak power directly generated by these mode-locked laser sources is often insufficient for studies of nonlinear phenomena. Several amplification techniques have recently been developed to extend the available pulse energies in the microjoule to millijoule range. However, the requirement of multiple stages of lasers makes these oscillator-plus-amplifier systems complex and expensive. Further, the repetition rate in kHz range from many of these sources is low enough to limit detection sensitivity for ultrafast measurements. Cavity dumping maintains the performance advantages of mode-locked lasers in terms of stability, tunability and pulse duration, while providing a significant increase in intensity of laser oscillators at variable repetition rates; but it is still a relatively complex technique because it requires the use of active devices.

Extended cavity and novel laser designs: For this contract, we have studied long cavity geometry for decreasing the pulse repetition rate from a laser oscillator. This long laser represents a complementary concept to scaling laser designs to shorter cavity lengths and compact sizes to achieve high repetition rates. In this case, the objective is to increase the laser output pulse energies and intensities by increasing cavity lengths. Since the total average output power of the laser cannot be increased, the pulse energy has been increased by reducing the repetition rate. The development of a long cavity femtosecond laser requires careful design because the laser cavity must be operated in a particular subset of its stability region for optimum Kerr lens mode-locking (KLM) performance.

As an approach to developing a long cavity laser, we have explored a Herriott-style multiple pass cavity (MPC) [1]. This device has been used for spectroscopy of gases where long optical propagation paths in a gas cell are required. The cavity length of our laser is extended by an MPC, which is used for optical delay lines as well as a unity q parameter transformation. This allows the cavity length to be increased while keeping the KLM operating point nearly invariant. The MPC is constructed by a pair of curved mirrors separated by a given distance. Both mirrors have notches cut in them in order to introduce and extract the optical beam. The optical beam is introduced into the MPC so that it strikes the first mirror off center and subsequently bounces between the two mirrors in a circular pattern, and it can be extracted after a given number of passes. The beam is also focused on subsequent bounces so that its propagation resembles

propagation through a periodic lens array. This device is designed such that it provides a unity transformation of the q parameter of the laser beam after a given number of transits. Thus, if this device is inserted into the KLM laser, it can have a zero effective length and leaves the laser cavity mode and nonlinear focusing behavior invariant.

We have completed preliminary investigations of a long cavity laser design using the MPC. Following this approach, we designed a high peak power laser using a standard, dispersion compensated KLM Ti:Al$_2$O$_3$ oscillator with an MPC incorporated into one of the arms (Figure 5.1). The projected performance of long cavity lasers is extremely attractive. Operation at 15 MHz repetition rate was achieved using a design in which the beam made 20 round trips between the MPC mirrors separated by 82.4 cm [2]. Stable mode-locking was achieved resulting in 0.7 MW peak power and 16.5 fs nearly transform- limited pulses. Lower repetition rates of 7.2 MHz were achieved using 24 round trips between the MPC mirrors separated by 148 cm [3]. We obtained 21 nJ output
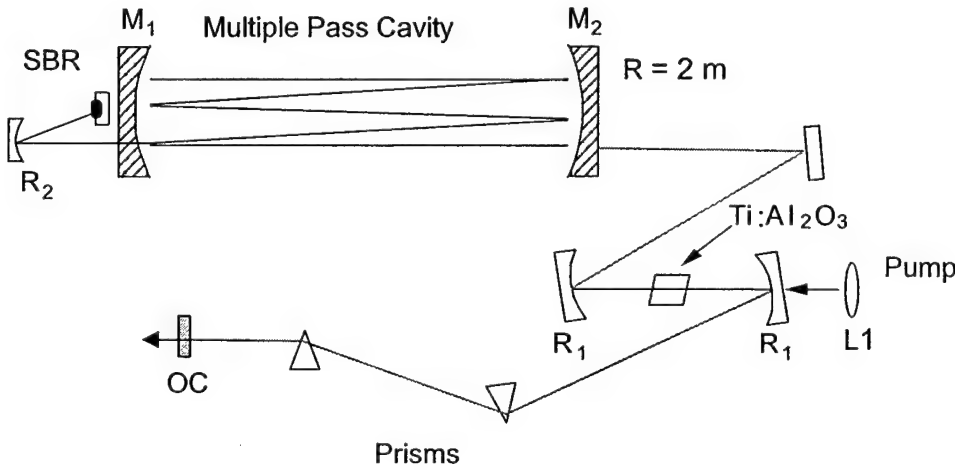

Figure 5.1: Schematic of long cavity, high power Ti:Al$_2$O$_3$ laser. The multiple pass cavity mirrors are: M1, M2, 2" diameter MPC mirrors with R=2 m radius of curvature; R1, R2, 10 cm radius of curvature mirrors; L, 6.3 cm focal length pump beam focusing lens; OC, 27 % ½" thick output coupler; Prisms, fused silica prisms.
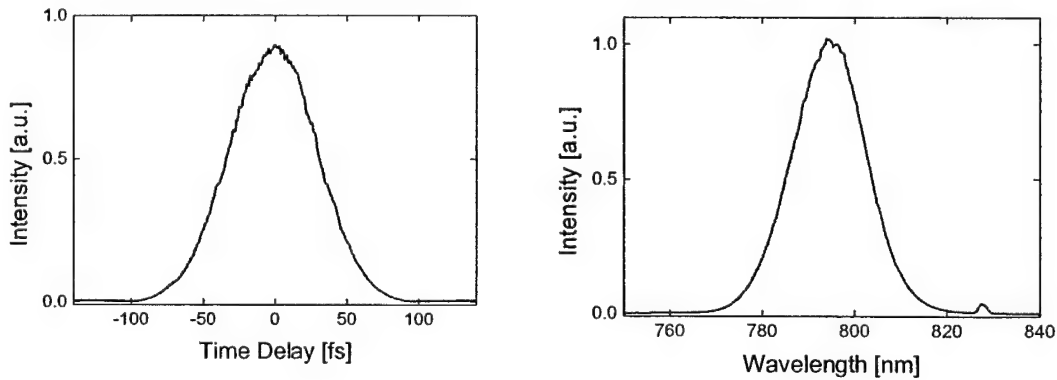

Figure 5.2: (a) Intensity autocorrelation trace showing a pulse duration of 44 fs assuming a sech$^2(t)$ intensity profile, (b) associated spectrum bandwidth of 19 nm from the KLM Ti:Al$_2$O$_3$ laser.

14

pulse energy in the two output beams and 23.5 fs nearly transform limited pulses, with a peak power of 0.9 MW. At a 5 MHz repetition rate, the beam makes 32 round trip passes between the MPC mirrors separated by 161 cm. Stable 60 nJ pulse energies with 44 fs nearly transform-limited pulses and a peak power of 1.4 MW were obtained (Figure 5.2). Commercially available typical mirrors would impose high losses from the large numbers of passes in the MPC. Thus, designs with large number of passes are not experimentally viable unless extremely low loss mirrors are used. In order to increase the reflectance of the MPC mirror, low loss TaO_2/SiO_2 standard quarter-wave mirrors are used. Since the reflectance of the MPC mirror is approximately 99.95% as a result of low scattering loss, its overall loss from 32 passes is less than 3%. The dispersion from air of 60m long cavity length in long lasers is compensated by an increasing prism separation.

Negative and positive dispersion modelocking with saturable Bragg reflectors: Achieving high pulse energies requires a detailed understanding of the KLM mechanism and the cavity operation because, as the laser cavity length is increased, the intracavity pulse energies and intensities are also increased to higher levels than in standard lasers. Thus, in order to avoid saturation of self-amplitude modulation effects due to high intensity pulses, the operating point of the laser must be adjusted. It is interesting to note that the critical power for self focusing is not a fundamental limit because this laser uses extremely a short gain crystal with a ~3 mm length. Thus, the self-focusing due to the optical Kerr effect occurs in a thin rather than a semi-infinite medium.

It is difficult to reduce pulse repetition rates because the peak pulse intensity increases to produce multiple pulsing instabilities or noises. This necessitates laser operation in a regime with a lower self-amplitude modulation, making the modelocking difficult to start. Thus, the starting mechanism for KLM should be decoupled from steady state mode-locked operation. To assist starting and to stabilize the laser against multiple pulsing formation, a saturable Bragg reflector (SBR) is incorporated in the laser. Since it is hard to start mode locking in the single pulsing regime as the total cavity length is long, the use of the SBR was essential to obtaining stable mode locking operation with long cavity lengths. The structure of the SBR consists of an $AlAs/Al_{0.85}Ga_{0.15}As$ quarter-wave dielectric stack grown by molecular beam epitaxy and a single GaAs quantum well.

In general, negative dispersion modelocking generates stable transform-limited pulses, which leads to high pulse intensities. However, using this scheme in the long laser has disadvantages because high pulse intensities cause instabilities from very high nonlinearities. However, as we increase net positive dispersion in KLM, positive chirp rapidly grows and laser pulses are significantly broadened in time [4]. These long chirped pulses can contain high pulse energies because the pulse intensity is significantly lowered inside the laser and the overall intracavity nonlinearity is also decreased. Since the chirped pulses have several picosecond durations, femtosecond pulses can be obtained from compensating positive chirp by an external prism compressor. The chirp of the pulse in this regime is nonlinear, which is potentially very hard to eliminate using a prism compressor only. Thus, after the prism compressor, the pulse cannot be transform-

limited. Positive dispersion KLM can potentially generate less than 30 fs transfom-limited pulses, when carefully designed chirped mirrors, gratings, and prism compressors are externally combined to compensate chirp.

Conventional femtosecond laser oscillators are operated in KLM with net negative group-delay dispersion. Hence, we at first explored negative dispersion modelocking with the SBR at different laser repetition rates. The best performance in preliminary studies is given by the laser operated at a 5 MHz repetition rate in which the beam made 32 round trips between the MPC mirrors separated by 161 cm. Mode locking is initiated by slightly moving the focal point of the curved mirror R2 onto the SBR or by shaking a prism. Stable KLM pulses are obtained at a 5 MHz repetition rate and the KLM region changes slightly from the 100 MHz laser. Cavity alignment was insensitive to changes in the separation for a pair of MPC mirrors. At 5.0 W pump power, we obtained 60 nJ pulse energy without any detrimental effects and 44 fs nearly transform limited pulses. Thus, the peak power was 1.4 MW and the mode-locked laser pulse train has 200 ns pulse interarrival time (Figure 5.3).
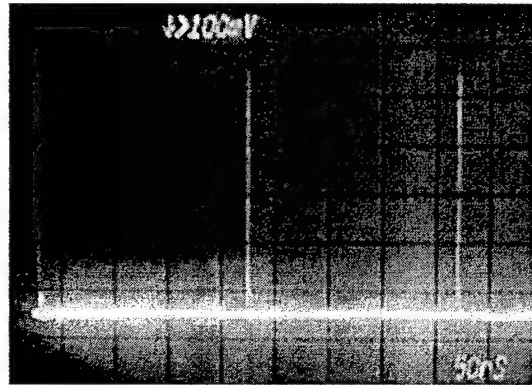

Figure 5.3: Mode-locked laser pulse train of 5 MHz repetition rate or 200 ns pulse interarrival time at 50 ns/div.

Interestingly, the pulse duration and the associated spectrum do not depend on whether the laser generates a single pulse or multiple pulses. The time-bandwidth product is 1.26 assuming a $sech^2(t)$ intensity profile; this suggests a gaussian temporal profile predicted by the pulse shaping mechanism of dispersion-managed solitons [5]. Also, modelocking was achieved without using the SBR but it always generated multiple pulsing with 46 nm spectrum bandwidth in the net negative dispersion regime. The associated pulse duration was nearly 20 fs with large noise in a pedestal. We believe that multiple pulsing is generated by insufficient saturable absorption and by the saturation of self-amplitude modulation, which facilitated starting without using the SBR.

Just above 5.0 W pump power, the laser suddenly starts to generate amplitude noise ~ 15 dB higher than that for low pump power. A significant pedestal increase has been measured from a background free intensity autocorrelation. With increasing pump energy, the pedestal level increases as well as the pulse energy. This behavior can be explained by saturated stabilization effects of the self-amplitude modulation against

16

multiple pulsing instabilities, because high intensity laser pulses drive the KLM with overly high nonlinearities. Thus it is crucial to decrease nonlinearities for obtaining stable higher pulse energies, which can be performed by decreasing laser pulse intensities inside the long laser oscillator.

From net positive dispersion KLM, operation at 4 MHz repetition rate was achieved using a design in which the net dispersion became positive with highly dispersive LaFN28 prisms instead of fused silica prisms. The beam made 50 round trips between the MPC mirrors separated by 129 cm in a slightly different configuration for the unity q transformation. Stable modelocking was achieved resulting in 100 nJ pulse energies and 80 fs pulses after the prism compressor to eliminate the positive chirp (Figure 5.4).
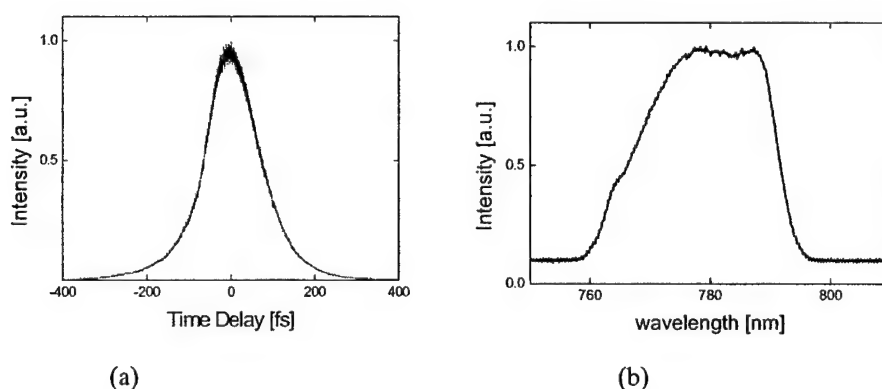

(a)   (b)

Figure 5.4: (a) Intensity autocorrelation trace showing a pulse duration of 80 fs assuming a $\text{sech}^2(t)$ intensity profile, (b) associated spectral bandwidth of 25 nm from the KLM Ti:Al$_2$O$_3$ laser.

References for Section 5

1. D. Herriott, H. Kogelnik, and R. Kompfner, Appl. Opt. 3, 523-526 (1964)
2. S. H. Cho, B. E. Bouma, E. P. Ippen, and J. G. Fujimoto, "Low-repetition-rate high-peak power Kerr-lens mode-locked Ti:Al$_2$O$_3$ laser with a multiple-pass cavity," Opt. Lett. 24, 417-419 (1999).
3. S. H. Cho, U. Morgner, F.X. Kaertner, E.P. Ippen, J.G. Fujimoto, J.E. Cunningham and W.H. Knox, in Conference on Lasers and Electro-Optics (Optical Society of America, Washington, D.C., 1999) paper CThR4.
4. H. A. Haus, J. G. Fujimoto, and E.P. Ippen, "Analytic theory of additive pulse and Kerr lens mode locking," J. Quant. Electron. 28, 2086-2096 (1992).
5. Y. Chen, F. X. Kartner, U. Morgner, S. H. Cho, H. A. Haus, E. P. Ippen, and J. G. Fujimoto, "Dispersion-managed mode locking," J. Opt. Soc. Am. B 16, 1999-2004 (1999).

6. Nonlinear semiconductor mirrors for femtosecond pulse generation

Nonlinear absorber elements for initiating, controlling and maintaining laser modelocking are playing an increasingly important role in ultrashort-pulse solid-state laser

technologies. The basic idea is that the nonlinear element needs to exhibit less loss for a short pulse than for low level cw radiation, but a variety of other more detailed properties determine the level of success with a particular laser system. Low gain lasers cannot tolerate very much insertion loss. An easily saturable loss may be desirable for initiating pulse formation but may not provide sufficient control over higher power steady state operation. The wavelength dependence of the nonlinearity and its dynamics limit the spectral width of the pulses, and the recovery time of the nonlinearity affects the saturability and determines how high a repetition rate is possible in the laser. To permit optimization of these various parameters in the design and fabrication of nonlinear absorbers we have focussed on epitaxially grown bulk and quantum-well absorbers on semiconductor mirrors. Realization of the absorbers we design is made possible by collaboration at MIT with Prof. Leslie Kolodziejski and her group.

The structures we have been designing and testing consist of InP-based absorber structures deposited by gas source molecular beam epitaxy on a distributed Bragg reflector (DBR). The DBR contained 22 pairs of quarter-wave AlAs/GaAs and produces >99% reflectivity over ~100 nm, centered at 1550 nm. The absorber layers, either bulk or quantum-well layers of InGaAs or InGaAsP, are imbedded in a nominally half-wave layer of InP which is grown epitaxially on the mirror top layer of GaAs. Since the device is operated on reflection and the fields inside the structure are standing waves, the interaction between the light and the absorber (i.e. both the linear absorption and the saturability) can be controlled by varying the position of the absorber within the half-wave layer. The bandgap and thickness of the absorber can be varied, the response time can be changed by strain in the InP layer or by subsequent proton bombardment, and additional dielectric reflection or anti-reflection coatings can be added to control the relative intensity in the absorber. Two of these structures are illustrated schematically in Figures 6.1 and 6.2.

To evaluate and study the nonlinear dynamics of these absorbers we perform measurements of reflectivity versus incident fluence using femtosecond pulses from a synchronously pumped optical parametric oscillator at wavelengths near 1550 nm. A typical result of such a fluence measurement is shown in Figure 7.3. As the fluence is increased the reflectivity of the mirror increases, consistent with absorber saturation. In this case the saturation fluence (the fluence at which the absorber is half bleached) is about 1 $\mu J/cm^3$. When the fluence is raised about 10 $\mu J/cm^3$ a very interesting and unexpected feature occurs.[1] By performing a variety of experiments we have confirmed that this is due to the onset of two-photon absorption in the InP cladding layer. The pump-probe trace insets in Figure 7.3 also illustrate this by revealing how instantaneous two-photon absorption dominates over the initial bleaching at high fluences. . The pump-probe response at low fluence reveals a fast recovery time of 350 fs and a slow time constant of 32 ps.
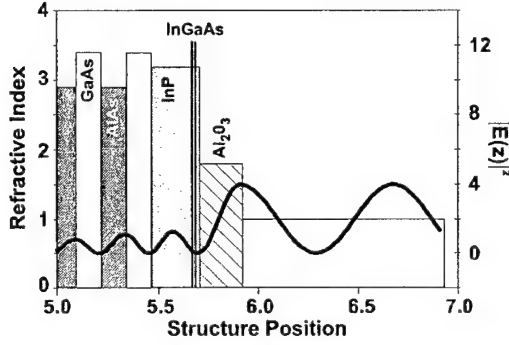
18

Figure 6.1: An anti-reflection coated saturable reflector with the InGaAs quantum wells near minimum field.
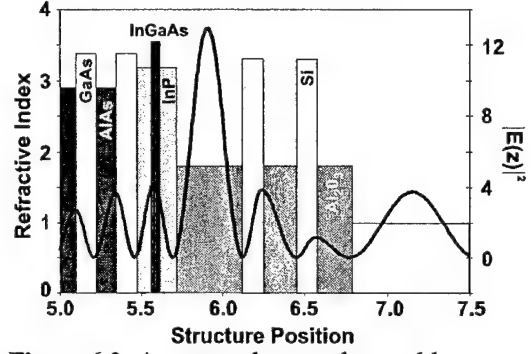

Figure 6.2: A resonantly coated saturable reflector with InGaAs quantum wells at maximum field.

We have carried out theoretical work that shows that this induced nonlinear absorption can play an important role in stabilizing modelocking and suppressing Q-switching in laser. [2] Since these aspects often depend also on the nonlinear dynamics of these absorbers at high fluences we have performed a series of pump-probe experiments over a range of even higher fluences.[3,4] They show the effects not only of two-photon absorption but of nonlinear free-carrier absorption and anomalous hot carrier relaxation rates. These detailed diagnostics now provide the basis for future designs of nonlinear mirrors.
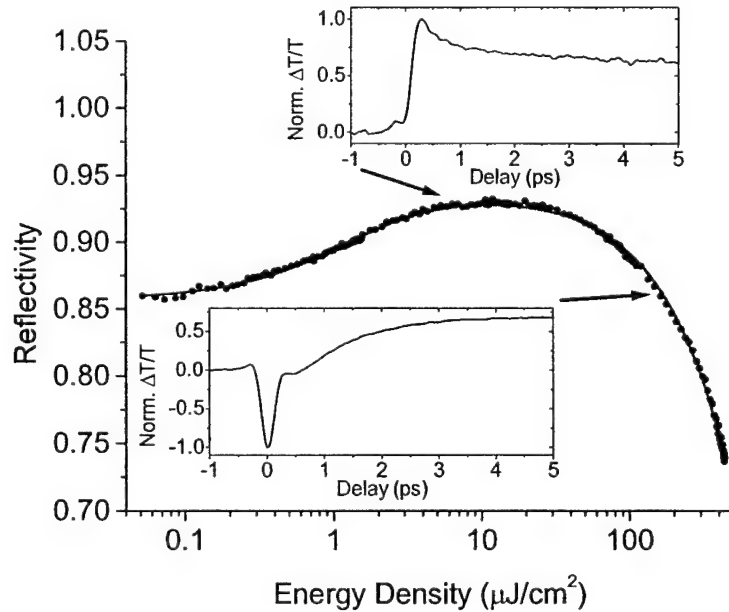

Figure 6.3: Reflectivity vs. fluence for a saturable absorber mirror showing bleaching at low fluences and instantaneous absorption at high fluences. Pump-probe trace insets illustrate the femtosecond dynamics at two different fluence levels.

19

Our ability to design, fabricate, characterize and use these absorbers in novel laser systems has been a unique strength of this program. It has also created opportunities to work with other university groups as well as industry in developing applications. Two examples of industry collaborations were IMRA (suppression of Q-switching) and Bell Laboratories (high rep-rate fiber soliton devices).

References for Section 6

1. E.R. Thoen, E.M. Koontz, M. Joschko, P. Langlois, T.R. Schibli, F.X. Kärtner, E.P. Ippen and L.A. Kolodziejski, "Two-photon Absorption in Semiconductor Saturable Absorber Mirrors," Appl. Phys. Lett. 74, pp. 3927-3929, 1999.
2. T. R. Schibli, e. R. Thoen, F. X. Kaertner, "Suppression of modelocked Q-switching and break-up into multiple pulses by inverse saturable absorption," to be published in Appl. Phys. B.
3. M. Joschko, P. Langlois, E.R. Thoen, E.M. Koontz, E.P. Ippen and L.A. Koldoziejski, "Ultrafast Hot-Carrier Dynamics in Semiconductor Saturable Absorber Mirrors, " Appl. Phys. Lett., 71, pp. 1383-1385, 2000.
4. P. Langlois, M. Joschko, E.R. Thoen, E.M. Koontz, F.X. Kärtner, E.P. Ippen and L.A. Kolodziejski, "High Fluence Ultrafast Dynamics of Semiconductor Saturable Absorber Mirrors, " Appl. Phys. Lett. 75, pp. 3841-3843, 1999.

7. Erbium glass waveguide lasers and short pulse generation

Erbium-ytterbium co-doped phosphate glass waveguides have recently been developed as an alternative to erbium-doped silica fiber because they offer the possibility of significant reduction in the device length needed for laser gain. This is a result of the higher doping densities possible in the phosphate glass. Er-Yb waveguides have exhibited more than 11 dB gain in 4.5 cm lengths [1] and can produce several hundreds of milliwatts outpower from these lengths. We have used such waveguide amplifiers in a fiber ring laser and generated 116 fs pulses with polarization additive pulse modelocking (P-APM) [2]. An important potential benefit of the waveguide technology, however, is shorter cavity lengths and therefore higher fundamental modelocking repetition rates. But, P-APM, which depends upon cumulative index of refraction nonlinearity, becomes less effective as the cavity length is reduced. Semiconductor saturable absorbers are a more logical choice for ultrashort pulse generation with short cavities. For short pulse generation via cw modelocking it also is necessary to suppress the tendency of the laser to Q-switch, a tendency that increases with short cavities and long upper state lifetimes. Thus compact waveguide lasers present a promising application for our semiconductor saturable absorber mirrors which can be engineered to exhibit both the saturability necessary for modelocking and the nonlinear absorption needed to suppress Q-switching.

The experimental arrangement used in our first studies of erbium-ytterbium waveguide laser modelocking with a saturable absorber mirror is shown in Figure 7.1. [3] The cavity contains a 5.2 cm Er-Yb waveguide (obtained through collaboration with TEEM

20

Photonics) with the intracavity facet at a 6° angle and the output face polished flat. At both ends of the waveguide fibers are butt-coupled with index matching fluid. A 15% transmitting dielectric coating was deposited on the fiber ferule butt-coupled to the flat waveguide facet providing an output coupler. The laser was pumped with 450 mW at 980 nm coupled in to the single-mode input fiber on the wavelength division multiplexer (WDM). A collimator at the output of the WDM collimates the laser light for polarization control, spectral filtering and focussing onto the nonlinear mirror.
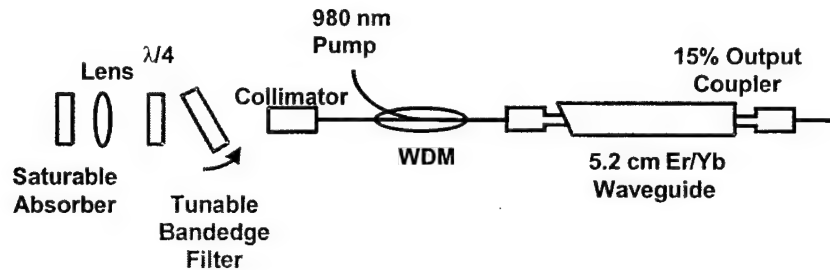

Figure 7.1: Schematic of the saturable absorber modelocked Er/Yb waveguide laser.

With the cavity configuration of Fig. 7.1 but without the filter, cw modelocking could be obtained consistently, if only at the narrow Er-Yb gain peak of 1534 nm. Relaxation oscillation sidebands were suppressed by 60 dB and the pulsewidths were on the order of 8 ps. The implications of the saturable absorber characteristics on this behavior are illustrated by Figure 7.2. The shaded region indicates the fluence range over which the laser operates in cw modelocked fashion (i.e. not Q-switched modelocked). In this range a pulse duration of 8 ps exists with minimum loss, as indicated by the dashed curve. The other reflectivity curves indicated, obtained experimentally for 150 fs pulses and extrapolated to 1 ps, indicates that shorter pulses would experience greater loss at the operating fluence.
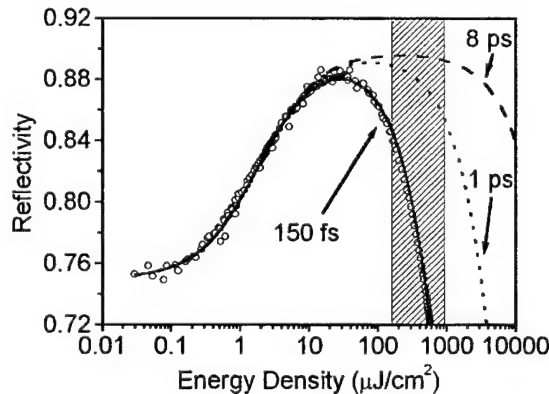

Figure 8.2: The semiconductor mirror reflectivity measured as a function of incident fluence with 150 fs pulses (circles). The solid line fit determines the saturable absorption and two-photon absorption parameters. The dotted and dashed lines indicate the expected reflectivity curves for 1 ps and 8 ps pulses respectively.

Another absorber with higher saturation (and TPA) fluence and with absorption extending to longer wavelengths was then used and a tunable bandedge filter was inserted and adjusted to push the spectrum away from the narrow gain peak to longer wavelengths. Pulses of 1 ps were obtained. This demonstrated that structures designed with proper absorption spectra and engineered values of TPA could be used to stabilize modelocking in lasers where it previously was not possible.

Erbium-ytterbium-doped waveguides offer a variety of opportunities for novel device fabrication and performance. Functions such as WDM waveguide coupling of the pump to the active guide, grating filters, mirrors and tapered coupling to fiber can be integrated on chip. Our ultimate goal is the development of very compact, high rep-rate, short-pulse sources. We are fortunate to have been able to obtain some of these unique structures through the generous collaboration of Denis Barbier of TEEM. We are also fortunate to have an excellent collaboration with Prof. Leslie Koloziejski's group through which we will be able to obtain the next generation of saturable absorber mirrors, designed for use with the erbium-doped waveguide amplifiers.

References for Section 7:

1. D. Barbier, M. Rattay, F. Saint Andre, G. Clauss, M. Trouillon, A. Kevorkian, J.-M. P. Delavaux and E. Murphy, "Amplifying four-wave combiner based on erbium/ytterbium-doped waveguide amplifiers and intergrated splitters," IEEE Photon. Technol. Lett. 9, 315-317 (1997)
2. D. J. Jones, S. Namiki, D. Barbier, E. P. Ippen and H. A. Haus, "116-fs soliton source based on an Er-Yb codoped waveguide amplifier," IEEE Photon. Technol. Lett. 10, 666-668 (1998)
3. E.R. Thoen, E.M. Koontz, D.J. Jones, D. Barbier, F.X. Kärtner, E.P. Ippen and L.A. Kolodziejski, "Erbium-Ytterbium Waveguide Laser Mode-Locked with a Semiconductor Saturable Absorber Mirror," IEEE Photon. Tech. Lett., 12, pp. 149-151, 2000.

8. Nonepitaxially grown saturable absorber devices for laser modelocking

In recent years ultrafast laser technology has advanced tremendously with the development of semiconductor saturable absorber devices. Previously, Kerr lens modelocking (KLM) was the most common method of ultrashort pulse generation. However, KLM is typically hard to align, not self-starting, and sensitive to external perturbations. Semiconductor saturable absorber devices, used for both fast saturable absorber modelocking and saturable-absorber assisted KLM, provide several advantages over KLM alone, including self-starting operation, simplicity in laser cavity design, and decoupling of the gain and modelocking mechanisms.

The most common saturable absorber technologies are semiconductor saturable absorber mirrors [1] and saturable Bragg reflectors [2], which have been extensively used for both saturable absorber modelocking and initiation of KLM. However, these devices require

epitaxial growth, which imposes lattice-matching constraints on the absorber materials and also requires complex and expensive systems for sample fabrication.

We have developed two simple and cost-effective alternatives to epitaxially grown saturable absorber devices. The first was the use of commercially available semiconductor-doped glasses as saturable absorbers [3]. These glasses have several attractive features for application to laser modelocking. They have fast carrier relaxation times and appropriate saturation fluences (~ 1 mJ/cm^2) while being simple and inexpensive. We polished Schott RG-830 and RG-850 glasses to a thin wedge, enabling us to vary the thickness of the glass introduced into a laser cavity. We then mounted the glasses on sapphire pieces and used the devices in a transmissive geometry to initiate KLM in a Ti:Al$_2$O$_3$ laser. The pulses were self-starting and 52 fs in duration. The semiconductor-doped glasses were also applied to fast saturable absorber modelocking without KLM, resulting in self-starting 2 ps pulses. We also investigated the nonlinear absorption saturation dynamics of these devices and observed a photodarkening effect that could impact the long-term performance of these devices when used in a laser cavity.

A second and more promising alternative to epitaxially grown saturable absorbers is the use of non-epitaxially grown semiconductor doped silica films as saturable absorber devices. These devices are fabricated by doping semiconductor nanocrystallites into silica films using rf or magnetron rf sputtering. RF sputtering is a simple and inexpensive technique that employs an argon plasma to eject material from a target which is then deposited onto a substrate. Magnetron rf sputtering improves deposition rates by confining the plasma to the target area.

Semiconductor doped silica films grown using rf or magnetron rf sputtering have several desirable features. They can be deposited on virtually any substrate, including oxides such as glass and dielectric coatings as well as metal mirrors. By varying the doping density of the semiconductor quantum dots, one can adjust the absorption coefficient of the device. A wide range of semiconductor materials can be doped into the silica films. Finally, appropriate choice of the semiconductor and knowledge of quantum confinement effects allow one to control the operating wavelength and absorption edge of the device.

Material fabrication and diagnostics: In our initial experiments we collaborated with Drs. James Walpole and Leo Misaggia of MIT Lincoln Laboratories in using a non-magnetron rf sputtering system to deposit silica films doped with InAs nanocrystallites. InAs was chosen as the semiconductor dopant due to its bandgap in the mid-infrared range. The sputtering target consisted of a 5 inch diameter disk of SiO$_2$ with wafers of InAs attached to it over 10% of its surface area. Films were deposited at 100 W rf power which resulted in a calibrated deposition rate of 20 Å/minute. The films were also subjected to a rapid thermal annealing (RTA) process which was found to tailor the absorption saturation dynamics of the devices.

The semiconductor-doped films were comprehensively characterized with measurements of nanoparticle size, film composition, element distribution within the film, and crystalline structure of the nanocrystallites [4]. X-ray photoelectron spectroscopy (XPS) measurements were performed to determine the

chemical composition of the InAs-doped silica films. From this we determined that indium and arsenic were present in the films in the form of InAs.

To determine the structural composition of the semiconductor-doped silica films, we performed transmission electron microscopy (TEM) and scanning transmission electron microscopy (STEM) experiments. From TEM experiments it was found that the films consisted of nanoparticles in a background matrix, with a large particle size distribution and maximum particle sizes of ~80 Å. Using STEM in conjunction with energy dispersive x-ray spectroscopy (EDX), the spatial distribution of elements within the film was examined. From Figure 8.1, it can be seen that In and As are concentrated in the same positions in the film, and these positions correspond to the nanocrystallites seen in the bright field image. Oxygen and silicon (not shown) are uniformly distributed throughout the film, as expected. Therefore, these measurements verify that the films consist of InAs nanocrystallites in a silica matrix.
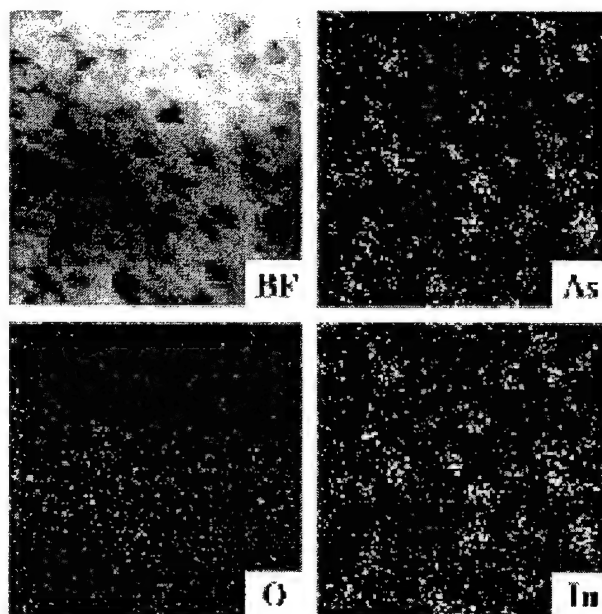

Figure 8.1: Transmission electron micrographs of rf sputtered InAs nanocrystallite film.

We also performed electron diffraction experiments to determine the crystalline structure of the InAs nanocrystallites. The material was found to be polycrystalline and it retained the zincblende structure of bulk InAs. The lattice constant was also measured and was comparable to the bulk InAs lattice constant.
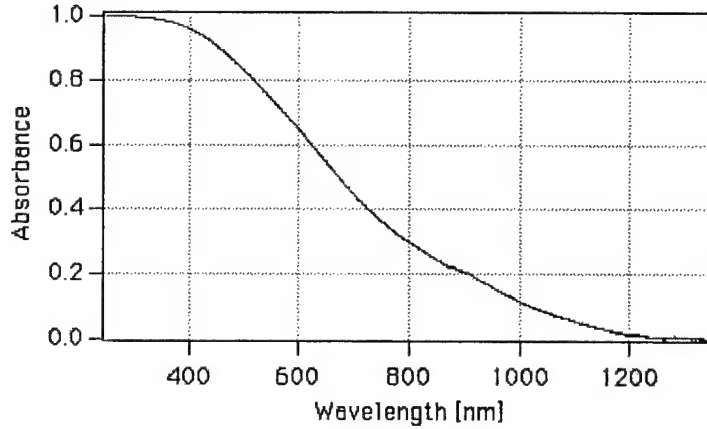
Figure 8.2: Absorption spectrum of rf sputtered InAs nanocrystallite film. Nanocrystallite-based devices can have significantly broader bandwidths than quantum well devices. The wavelength of operation can be adjusted by controlling the nanocrystallite size.

Characterization of linear and nonlinear optical properties: We measured the linear absorption characteristics of the semiconductor-doped silica films to verify that they provided optical absorption at the lasing wavelength of 800 nm (Figure 8.2). From this figure the optical absorption edge can be determined to be 1.2 μm. The smooth absorption characteristic is due to the broad size distribution of the InAs nanocrystallites and leads to a broad tuning range when the films are applied to laser modelocking.
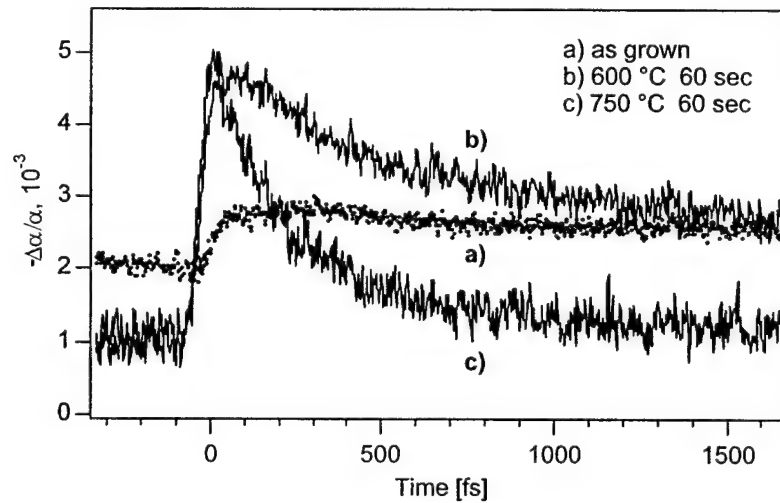

Figure 8.3: Pump probe measurements of rf sputtered films annealed at different temperatures.

We performed pump-probe measurements at 800 nm to characterize the nonlinear optical properties of the saturable absorber films (Figure 8.3). It was found that the RTA process reduced the saturation fluence of the films by a factor of two, making them more suitable for self-starting laser modelocking. However, the saturation fluence of the annealed films (25 mJ/cm^2) is still significantly higher than that of epitaxially grown

saturable absorber devices (typically 50 $\mu J/cm^2$), which limits the pulsewidth and does not enable saturable absorber modelocking without KLM. The absorption saturation recovery times also decreased with increasing annealing temperature.

Modelocking in solid state lasers: Saturable absorber films were fabricated for use in a transmissive geometry within a $Ti:Al_2O_3$ laser cavity[5]. The films were 300 Å thick to provide 2% absorption at the lasing wavelength and were deposited on a 0° oriented sapphire substrate to avoid birefringence effects. The devices were also annealed at temperatures of 600 and 750 °C for 60 seconds. The saturable absorber devices were introduced into a standard z-cavity $Ti:Al_2O_3$ laser containing a second fold with 5 cm and 7.5 cm radius of curvature mirrors
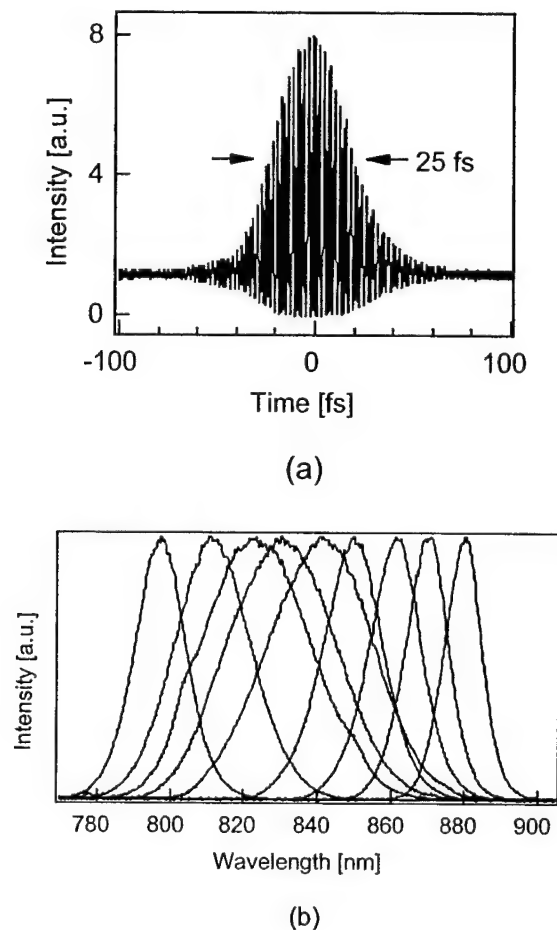

(a)

(b)

Figure 8.4: (a) Autocorrelation of a $Ti:Al_2O_3$ laser using a nanocrystallite film saturable absorber to start KLM; (b) Output spectra demonstrating the wavelength tuning range of the KLM laser.

in which the absorber was placed, oriented at Brewster's angle. In this configuration, self-starting 25 fs pulses were obtained (Figure 8.4(a)) with bandwidths of 53 nm. The pulses were not transform-limited due to excess self-phase modulation in the sapphire substrate. The wavelength could also be tuned from 800 to 880 nm while maintaining

26

self-starting operation as shown in Figure 8.4(b). This is believed to be the first demonstration of laser modelocking with nonepitaxially grown saturable absorber films.

The primary drawback of semiconductor-doped silica film saturable absorbers is their high saturation fluence, limiting the pulsewidth and making self-starting operation without KLM impossible; therefore, we have been examining several methods of decreasing the saturation fluence in these devices. One method is to design a reflective saturable absorber device incorporating semiconductor-doped silica films. A standing wave is formed in a laser cavity when an electromagnetic wave is reflected from a mirror; by placing the semiconductor-doped film at the peak of the standing wave, the effective saturation fluence can be reduced by a factor of four.

We have fabricated reflective saturable absorber devices in the rf sputtering system at Lincoln Laboratories. These devices are made by sandwiching a InAs-doped film between two sapphire spacer layers on top of a gold mirror, all deposited by rf sputtering. The thickness of the spacer layers can be modified to place the semiconductor-doped film at the desired point in the standing wave pattern. The devices were also annealed and found to preserve good optical quality. Pump probe experiments and application of these devices to $Ti:Al_2O_3$ laser modelocking in a reflective geometry are now underway.

In general, we expect films with larger nanocrystallites and greater purity to have a lower saturation fluence [6]. Magnetron rf sputtering offers advantages such as increased deposition rates and plasma confinement to the target area, which should lead to purer films. Currently we are investigating the influence of deposition parameters such as rf power, substrate temperature, and film composition on the linear and nonlinear optical properties of our semiconductor-doped saturable absorber films. Semiconductor-doped films incorporating both InAs and GaSb have been fabricated in the magnetron rf sputtering system with different deposition parameters and their linear optical properties have been characterized. We are also developing a new pump probe system using our 5 fs $Ti:Al_2O_3$ laser to characterize these films; this system will have the advantage of high time resolution as well as the ability to characterize the nonlinear optical response at different wavelengths. We propose to completely characterize the nonlinear optical properties of our devices as a function of different deposition parameters using this pump probe system. Using our knowledge of the linear and nonlinear optical properties of the semiconductor-doped silica films, we should be able to design semiconductor-doped silica film saturable absorber devices with appropriate saturation fluences and carrier relaxation times to obtain optimal self-starting performance in either a transmissive or reflective geometry. These devices could then be used to self-start modelocking of a $Ti:Al_2O_3$ laser with or without KLM. This technique can also be extended to different laser wavelengths by changing the nanocrystallite size or the semiconductor material doped into the silica films, making it a versatile and inexpensive alternative to epitaxially grown saturable absorbers.

References for Section 8

1. U. Keller, K. J. Weingarten, F. X. Kartner, D. Kopf, B. Braun, I. D. Jung, R. Fluck, C. Honninger, N. Matuschek, and J. A. d. Au, "Semiconductor saturable absorber mirrors (SESAM's) for femtosecond to nanosecond pulse generation in solid-state lasers," IEEE J. Selected Top. Quantum Electron., vol. 2, pp. 435-453, 1996.
2. S. Tsuda, W. H. Knox, S. T. Cundiff, W. Y. Jan, and J. E. Cuningham, "Mode-locked ultrafast solid-state lasers with saturable Bragg reflectors," IEEE J. Selected Top. Quantum Electron., vol. 2, pp. 454-464, 1996.
3. I.P. Bilinsky, R. P. Prasankumar, and J. G. Fujimoto, "Self-starting mode locking and Kerr-lens mode locking of a $Ti:Al_2O_3$ laser by use of semiconductor-doped glass structures," J. Opt. Soc. Am. B, vol. 16, pp. 546-549, 1999.
4. I. P. Bilinsky, J. G. Fujimoto, J. N. Walpole, and L. J. Misaggia, "InAs-doped silica films for saturable absorber applications," Appl. Phys. Lett., vol. 74, pp. 2411-2413, 1999.
5. I. P. Bilinsky, J. G. Fujimoto, J. N. Walpole, and L. J. Misaggia, "Semiconductor-doped silica saturable absorber films for solid state laser mode locking," Opt. Lett., vol. 23, pp. 1766-1768, 1998.
6. I. P. Bilinsky, Novel Saturable Absorber Materials and Devices for Laser Modelocking, Ph.D. thesis, MIT, Department of Physics, 1998.

9. Ultrashort pulse fiber devices

We have had considerable success in the invention and development of novel optical fiber lasers, optical data storage rings and switches [1,2,3,4]. With fiber lasers we have demonstrated the ability to produce either picosecond solitons at high (multi-GHz) repetition rates or femtosecond pulses in stretched-pulse systems at somewhat lower rates. Optical storage rings make use of our determining that pulse data packets (patterns) can be maintained indefinitely in a harmonically modelocked, high rep-rate ring laser. We have shown that switches and pulse selectors based on nonlinear fiber loop mirrors can be made sensitive to pulse shape as well as pulse intensity. Advances in any of these technologies depend upon better understanding of nonlinear propagation in fibers, pulse forming effects, pulse jitter and pulse pattern stabilization in fiber lasers. Our most recent work focuses on two experimental systems: an actively and harmonically modelocked soliton laser producing pulses of about one picosecond in duration, and a hybrid, active/passive system producing sub-picosecond pulses stabilized by active phase modulation.

Polarization maintaining fibers, harmonic modelocking and jitter reduction: Since fiber lasers require lengths of at least several meters of erbium-doped fiber for sufficient gain, GHz repetition rates require operation at high harmonics of the fundamental repetition rate. An active modulator is employed to divide the roundtrip period into multiple time slots and many pulses exist in the laser at the same time. Two potential problems in such a system are: pulse shortening by soliton effects and nonlinear polarization rotation that reduces the ability of the modulator to keep pulses in the synchronous time slots, and the possibility that the amplitude and timing of the pulses varies from time-slot to time-slot.

28

To study the first problem we constructed an actively modelocked fiber ring laser out of polarization maintaining fiber and performed measurements of pulse timing restoration with both amplitude modulation and phase modulation at a high harmonic of the cavity roundtrip frequency [5].
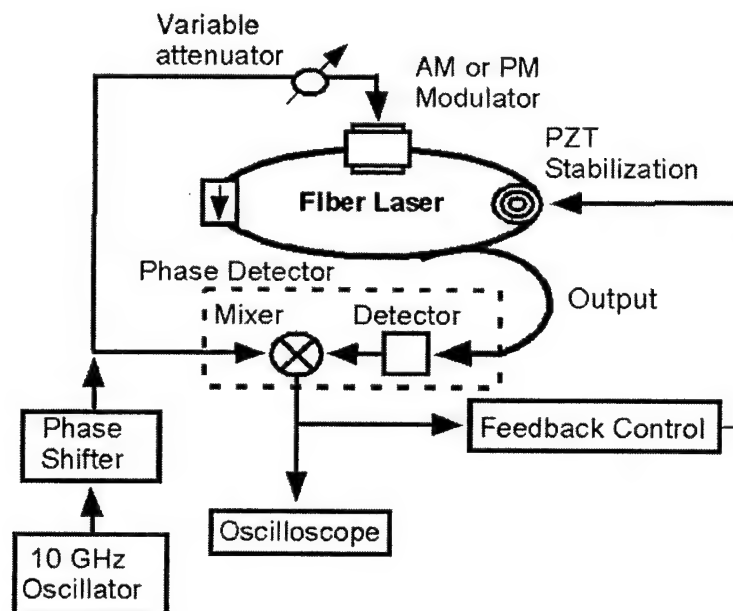

Figure 9.1: Fiber ring laser for timing studies.

The laser we have developed is shown in Figure 9.1. The fiber laser is 167 meters long-- corresponding to a 1.2 MHz free spectral range (833 ns round trip time)--and constructed with polarization-maintaining fibers. The pulsewidth can be varied from 1.5 to 3.5 ps by changing the pump power and modulation depth. The rf synthesizer is set to the frequency of the cavity harmonic closest to 10 GHz, and suppression of the supermodes is greater than 65 dB. The laser pulse train is detected with a photodiode (45 GHz electrical bandwidth), and the phase of the fundamental component is compared to the rf synthesizer driving the modulator, generating an error signal. The error signal is integrated and amplified to drive a fiber-wound PZT that changes the length of the laser cavity, completing a phase-locked feedback loop that ensures stable active modelocking. By applying an instantaneous perturbation to the phase of the rf synthesizer driving the laser and opening the feedback circuit—achieved in practice by reducing the bandwidth of the feedback circuit to less than 2 Hz, so as to maintain stable modelocking during repeated measurements—we obtain the transient retiming dynamics at the output of the phase detector.

The theory we developed predicts that the timing recovery for amplitude modulation (AM) should exhibit an exponential recovery proportional to the length of the laser and inversely proportional to the product of the modulation depth and square of the pulsewidth. For phase modulation (PM), the timing recovery is described as that of a damped harmonic oscillator.

Traces of the retiming dynamics after an instantaneous phase shift for AM are shown in Figure 9.2a for two different modulation depths. The dashed and dashed-dot lines are fits to an exponential decay. The recovery times for the two traces are 45 and 175 μs, corresponding to 54 and 210 round trips, respectively. A series of such traces was taken for various values of modulation depth, and the recovery time was extracted for each corresponding exponential fit. The measured time constants for AM are in excellent agreement with the theory.

In contrast to the case of AM, timing is not restored directly by PM. Mistimed pulses first experience a shift in frequency that converts to retiming through group-velocity dispersion (GVD). Upon successive round trips, the accumulated frequency shifts are damped out by filtering. Two typical traces are shown in Figure 9.2b, one corresponding to the underdamped case (where the modulation depth is large) and another where the retiming follows a trajectory closer to that for critical damping (where the modulation depth has been reduced). The curve fits correspond to a damped harmonic oscillator with two free parameters. The measured time constants are again in excellent agreement with the theory: timing recovery for PM is governed by two time constants, one governing damping, and another governing oscillation.
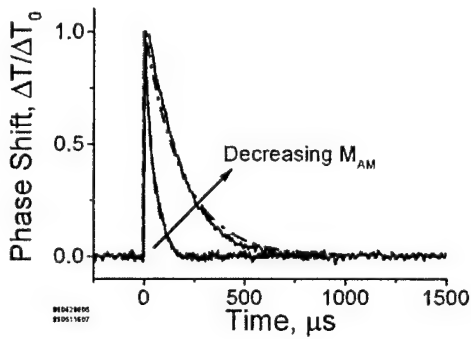

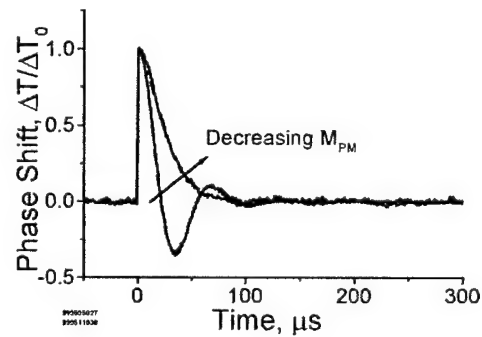**Figure 9.2a:** Timing recovery following a step-wise excitation, amplitude modulation.

Figure 9.2b: Timing recovery following a step-wise excitation, phase modulation.

Application of this type of laser to technologies requiring very low noise, precise timing and jitter control now requires careful measurement of these quantities and development of a theory relating them to the results above and further optimization of the laser parameters. Our preliminary results indicate that the minimum jitter for AM requires dispersion management in which the local dispersion swings between anomalous and normal but the net dispersion is near zero. This reduces the jitter due to frequency fluctuations while enhancing the pulse energy. For PM, the minimum jitter requires an optimum dispersion because large dispersion increases the timing recovery from noise that comes from timing fluctuations, but dispersion also increases the noise that comes from frequency shifts via the Gordon-Haus effect.

Supermode control and two-photon absorption: Active harmonically mode-locked fiber lasers producing picosecond pulses at gigahertz repetition rates for communications and

precision optical sampling require a mechanism to equalize pulse energies to prevent amplitude fluctuations and pulse dropouts. As discussed in Section 6 it has been shown that two-photon absorption (TPA) can limit the peak intensity of Q-switched mode-locking and enhance the stability of continuous-wave mode-locking. In very recent experiments [6] we have also shown that a semiconductor mirror providing TPA in a harmonically mode-locked fiber laser introduces a fast intensity-dependent loss that can equalize pulse energies and reduce pulse dropouts.
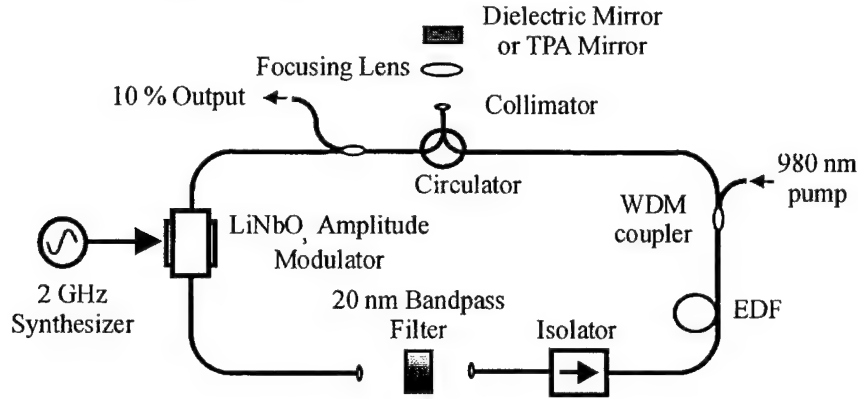

Figure 9.3. Laser setup for nonlinear supermode control all fibers are polarization maintaining.

Figure 9.3 shows how we have introduced such a nonlinear mirror into a fiber ring laser using a circulator. An aspheric lens is used to produce a small spot size ($\sim 5 \times 10^{-8}$ cm^2) on the mirror. To test the laser operation without TPA, a dielectric mirror (> 99.9% reflectivity at 1.55 µm) was used in this position. Autocorrelations yielded transform-limited 1.8 ps pulses at 1.555 µm. The rf spectrum exhibited 25 dB supermode suppression, as shown in Figure 9.4a, indicative of occasional dropouts. Figure 9.4b shows a digital oscilloscope scan over a long time scale (tens of ns) as compared to the repetition rate (500 ps), verifying that pulses are missing. Note that individual pulses are not resolved due to the limited resolution of the oscilloscope.
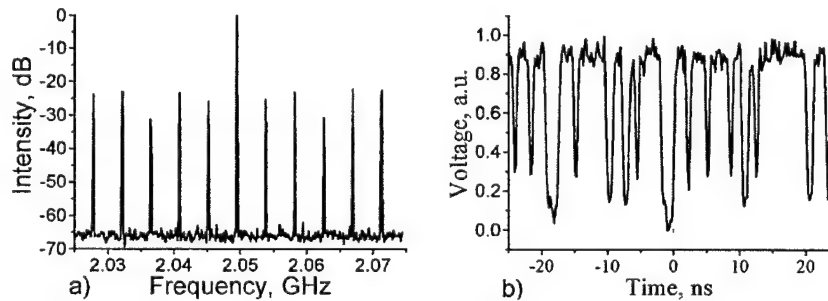

Figure 9.4: Laser output without the TPA mirror. a) Rf power spectrum, 3 kHz resolution bandwidth, and b) Digitizing oscilloscope trace.

The dielectric mirror was replaced by a TPA mirror, and with the average power held constant, the laser produced pulses of similar duration. The TPA mirror consists of a ~5.1 μm InP layer deposited via gas source molecular beam epitaxy onto a 22 period GaAs/AlAs distributed Bragg reflector (>99% reflectivity at 1.55 μm). A dielectric antireflection coating was deposited on the front surface. TPA introduces an instantaneously greater loss for higher peak intensity, which suppresses amplitude fluctuations and pulse dropouts by favoring a filled pulse train of low-intensity pulses over a partially filled pulse train of high-intensity pulses. The supermode suppression was enhanced by 30 dB (compared with Figure 9.4a), and the corresponding oscilloscope trace in Figure 9.5b reveals the absence of pulse dropouts. Based on nonlinear reflectivity measurements of a similar structure and the incident peak intensity, the nonlinear loss of the TPA mirror was estimated to be between 0.5 and 1%. To verify the intensity dependence of the TPA effect, the peak intensity on the TPA mirror was lowered dramatically by removing the focusing lens (spot size ~ 9.5×10^{-3} cm^2), yielding results similar to those of Figure 9.4.
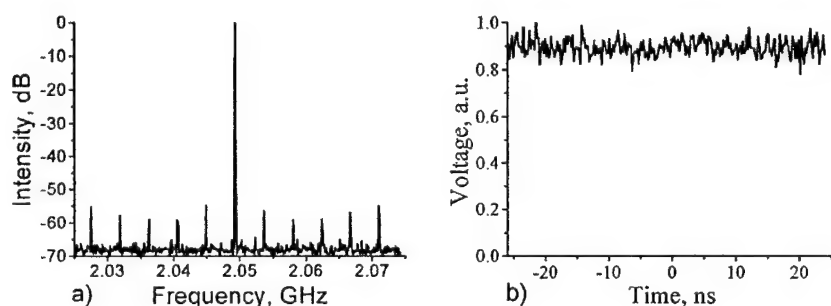

Figure 9.5: Laser output with the TPA mirror and focusing lens. a) rf power spectrum, 3 kHz resolution bandwidth, and b) Digitizing oscilloscope trace.

Some of the novel potential features of TPA-assisted harmonic mode-locking are the operation of environmentally stable, short laser cavities; the opportunity for specific tailoring of semiconductor materials and waveguide structures for optimum performance and integration; and laser operation even in the non-soliton regime. We intend to investigate each of these possibilities.

Synchronized passive modelocking with a phase modulator: The generation of pulses with ultrabroad spectra creates pulses at many different wavelength channels simultaneously. Passively modelocked fiber lasers have been used previously for producing femtosecond pulses and broad spectra, but the repetition rates have been low and they have not been synchronized to a reference clock. Active modelocking has provided GHz rep-rates and permits locking to a drive signal, but has only produced picosecond pulses. Adding a modulator to a passively modelocked laser has the potential to combine the best features of both types of systems. We have shown recently that this can be accomplished if one uses phase modulation [7].
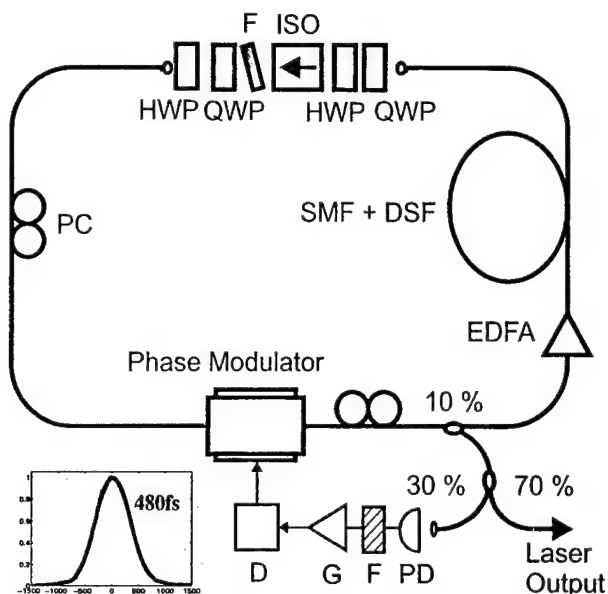
Figure 9.6: Laser Schematic, HWP: Half Wave Plate, QWP: Quarter Wave Plate, D: Phase Delay line, G:RF amplifier, F:1GHz Filter, PD: Photodetector. Inset: Autocorrelation, FWHM=480fs.

This laser is illustrated in Figure 9.6. The passive modelocking mechanism is polarization additive pulse modelocking (P-APM). Part of the laser output is used to drive the phase modulator. The rf and the optical spectra of the output when the modulator is on are shown in Figure 9.7 (a) and (b). The sidemode suppression is >60dB and the spectral FWHM is 5.6 nm. Figures 9.7 (c) and (d) show the rf and optical spectra when the modulator is off. The absence of the feedback leaves the pulses in random time slots but the envelope of the optical spectrum remains unchanged. Thus, P-APM shapes the pulses and the modulator synchronizes them and prevents dropouts. The pulsewidth in both cases is 480 fs, much shorter than that achievable with the modulator alone. This mode of operation is quite remarkable and not entirely expected. We intend to investigate its potential further, determining the noise and jitter properties as well as its ability to generate shorter pulses and higher rep-rates.

Broadband generation: To generate even broader spectrum, the output of this laser is amplified by a double-clad Er/Yb fiber amplifier and 4.5m of dispersion compensating fiber (DCF) compensates for its dispersion. The hexagonally shaped amplifier fiber from Lucent Technologies has a diameter of 130 μm and and NA of 0.45. The spectrum broadens to 9.1 nm and the pulse shortens to 304 fs. Then the amplifier output is sent into dispersion decreasing fiber (DDF). The spectra before and after the DDF are shown in Figure 9.8. The upper spectrum is generated with an input power of 200 mW and is asymmetric. But the spectral intensity within the central 80 nm varies by no more that 6 dB. Even broader spectra have been obtained at higher input powers though they are less smooth.
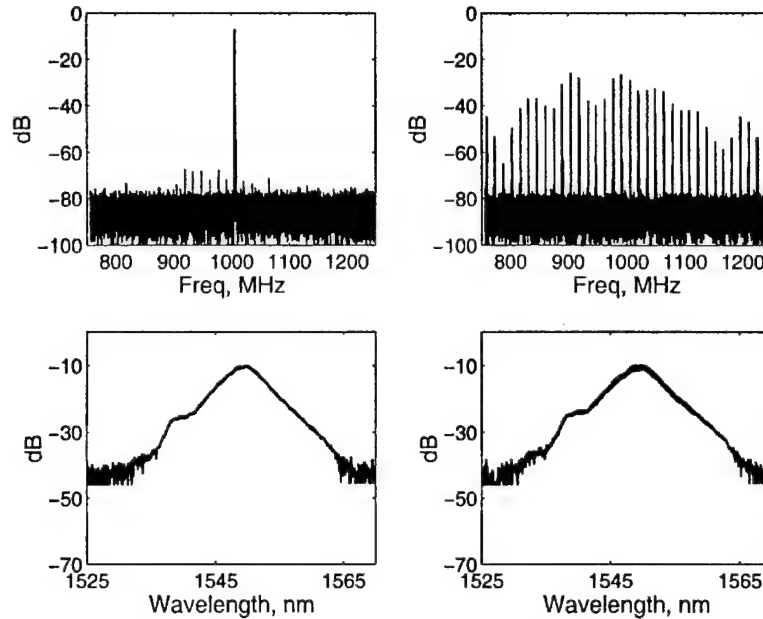
33

Figure 9.7: Output of the laser: rf spectrum optical spectrum when the modulator is on (left), rf spectrum and optical spectrum when the modulator is off (right). The RBW of the rf spectrum is 100KHz, and the RBW of the optical spectrum is 0.5 nm. The suppression in (a) is >60dB. The spectral width is 5.6 nm in both cases.
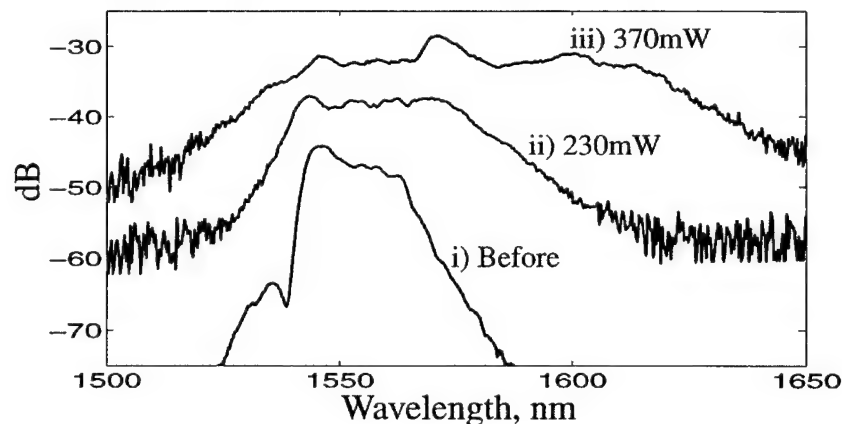

Figure 9.8: Unaveraged spectra before and after broadening in a dispersion decreasing fiber at two different power levels.

References for Section 9

1. E.P. Ippen, D.J. Jones, L.E. Nelson and H.A. Haus, "Ultrafast Fiber Lasers," Ultrafast Phenomena XI, Chem. Phys. Vol. 63, pp. 30-34, Springer Verlag, November, 1998.
2. D.J. Jones, H.A. Haus, L.E. Nelson and E.P. Ippen, "Stretched-Pulse Generation and Propagation", IEICE Trans. Electron. E81-C, pp. 180-188, 1998.
3. D.J. Jones, K.L. Hall, H.A. Haus and E.P. Ippen, "Asynchronous Phase-Modulated Optical Fiber-Ring Buffer", Optics Lett. 23, pp. 177-179, 1998.

4. E.P. Ippen, D.J. Jones, W.S. Wong, L.E. Nelson and H.A. Haus, "Fiber Devices for Ultrahigh-Speed Photonics," Trends in Optics and Photonics, Vol. 23, H.A. Haus, ed., Optical Society of America, January, 1999

5. M.E. Grein, L.A. Jiang, Y. Chen, H.A. Haus and E.P. Ippen, "Timing Restoration Dynamics in an Actively Mode-Locked Fiber Ring Laser," Optics Lett. 24, pp. 1687-1689, 1999.

6. M.E. Grein, E.R. Thoen, E.M. Koontz, H.A. Haus, L.A. Kolodziejski, and E.P. Ippen, "Stabilization of an Active Harmonically Mode-Locked Fiber Laser Using Two-Photon Absorption," QELS 2000, San Francisco, CA, paper CME5, May 7-12, 2000.

7. C.X. Yu, W.S. Wong, H.A. Haus, E.P. Ippen, and A. Sysoliatin, "A GHz Regeneratively Synchronized Passively Mode-Locked Fiber Laser for Spectrum Generation in the 1.5-μm Region," QELS 2000, San Francisco, CA, paper CMP6, May 7-12, 2000.

10. Photonic device fabrication using nonlinear material processing

The rapid prototyping and fabrication of new photonic devices is important for the future development of ultrafast photonic technology. In particular, further miniaturization and integration of photonic devices is required in order to increase the density of the devices because of the rapidly increasing information capacities in optical communication systems. To achieve this objective, versatile fabrication techniques, which are both high precision as well as have the flexibility to fabricate different structures and optical materials, are required.

Glass materials have been widely used in photonic devices such as Bragg gratings. Glass materials have several advantages in that they are generally cost-effective, their characteristics are easy to be modified by doping of various components, and they are easy to connect to glass fibers, which are used in optical communication systems. Moreover, the photosensitivity of glass has been utilized to fabricate devices by optical processing. Optical processing techniques have several advantages over conventional fabrication approaches. The techniques for focussing and scanning light beams are well developed and different structures can be prototyped simply by altering the scanning patterns. Conventionally, glass waveguide devices have been fabricated by UV irradiation techniques; however, they have several fundamental limitations. Because of the requirement of high UV sensitivity, the types materials which can be processed are restricted. Fabricated device structures are limited in one- or two-dimension because of the shallow penetration depth of UV light. However, three-dimensionality is the key to achieving high integration in a device, and also enables greater flexibility in device design and fabrication. For example, it will be possible to fabricate several independent devices in different layers to increase density, or a waveguide device with three-dimensional structures that have more complex functions than possible in two-dimensions.

In recent years, many groups have been investigating and demonstrating the use of nonlinear interactions with near IR ultrashort pulses for ultraprecision microprocessing

and micromachining of various materials, such as metals, semiconductors, and glasses [1,2,3]. The effect of thermal diffusion into the surrounding material, which is inevitable in conventional techniques, is greatly reduced using nonlinear processes, and thus clean and well-controlled structures may be created. In the case of glass materials, these effects are especially evident. Unlike UV photosensitive exposure techniques which are mediated by linear absorption, irradiation using high-intensity, near-IR ultrashort pulses is mediated by multi-photon absorption. Thus, modification of the optical properties is possible in a wide range of glasses which may not have linear absorption sensitivity. The absence of linear absorption allows subsurface processing due to deep penetration. Also, the nonlinear nature of the interaction between irradiated light intensity and material modification gives localized structures in both transverse and longitudinal directions, because only at the focal point is there enough light intensity to make the effective modification. The deep penetration combined with the localization of the modified area is attractive for creating three-dimensional devices.

Although many groups have demonstrated the efficacy of these techniques for fabricating several types of devices, such as waveguides and gratings, there is a practical difficulty because expensive and complicated laser amplifier systems have been used to achieve high-intensity femtosecond optical pulses. Our group has developed a compact femtosecond laser oscillator using a novel design which generates high-intensity pulses directly, without the need for a laser amplifier or other complicated active devices (Chap. 6). Moreover, the higher repetition rate (MHz) of this laser compared to standard amplifier systems (kHz) enables faster and more efficient fabrication of devices. Very recently, processing of glass waveguides by using femtosecond oscillator pulses has been reported [4]. In that study, the pulse energy is just above the threshold of the material modification (around 10 nJ), and thus only very tight focusing of the beam enables processing. Our laser can generate significantly higher pulse energies (100 nJ), far above the threshold for nonlinear exposure. This enables greater flexibility in fabrication parameters, such as irradiation laser power, focus, and processing speed. Such flexibility is crucial to fabricate complex devices, because precise manipulation of structures and optical properties is required. We propose to develop ultrashort pulse materials processing techniques and apply them for the investigation and development of new photonic devices.

Waveguide fabrication and characterization: As a starting point for this project, we will investigate one-dimensional passive waveguides in glass since these are one of the most basic devices. We have begun preliminary studies of waveguide fabrication and characterization by irradiation of pulses of 100 nJ energy and 80 fs duration from a 4.2 MHz repetition rate, KLM Ti:Al_2O_3 laser oscillator. Figure 10.1 shows a schematic of the fabrication system. Changes in material optical properties were produced using high intensity ultrashort pulse exposure by tightly focusing the pulses using a microscope objective (63 X Achroplan) inside a glass slide. Then, a waveguide structure was formed by translating the glass sample perpendicular to the incident light while exposing with multiple pulses at MHz repetition rate.
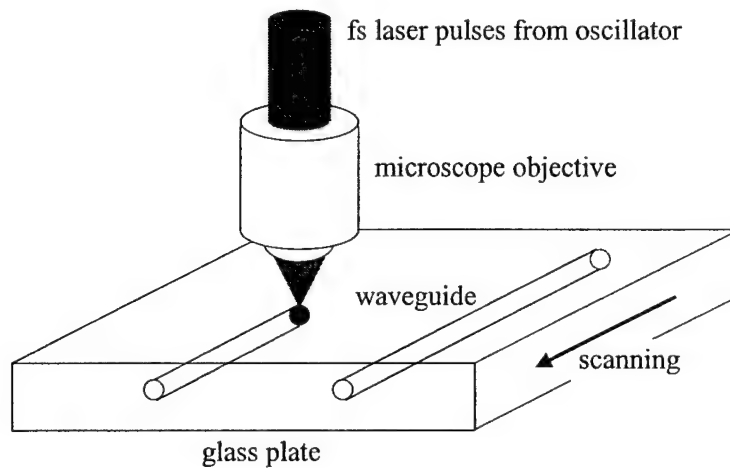
Figure10.1: Schematic of the fabrication system. Modification area was made by tightly focusing the pulses using a microscope objective (63 x Achroplan) inside a glass slide. Then a waveguide structure was formed by translating the glass sample perpendicular to the incident light exposed to multiple shots.
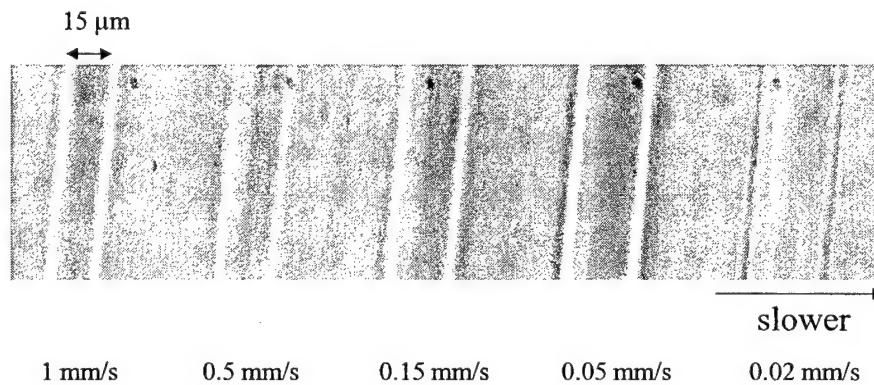

Figure 10.2: Top view of several widths of waveguide structures fabricated inside BK7 glass by changing scanning speed.

Preliminary studies demonstrated that waveguide dimensions could be controlled by changing the incident power or the exposure translation speed. Figure 10.2 shows top view of several different waveguide structures with different widths fabricated inside BK7 glass by the changing the exposure scanning speed. When those parameters were properly selected, we could achieve a single mode waveguide. Figure 10.3 shows an image of cw Ti:Al$_2$O$_3$ laser beam which is guided into a waveguide of 1 μm width. The image was taken at the output of the waveguide using a CCD camera. The single mode nature of the guided beam is evident. In contrast, when the incident power for the exposure was high, concentric double structures were observed. We believe that the laser ablation occurred at the center and void structures were fabricated. This result is significant because laser ablation has not been previously reported using only the unamplified output of a femtosecond laser oscillator.
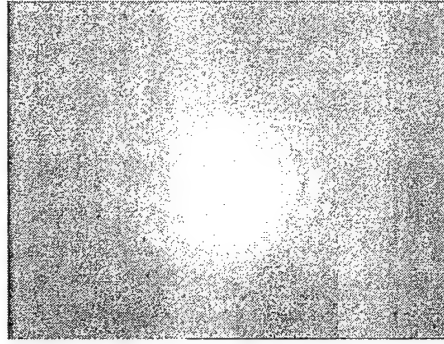
Figure 10.3: Image of cw Ti:Al$_2$O$_3$ laser beam which is guided into a waveguide of 1 μm width. The image was taken at the output of the waveguide by CCD camera. Single mode nature of the guided beam is observed.

In addition to waveguide mode measurements, we can also apply optical coherence tomography (OCT) and other high sensitivity diagnostic imaging techniques to characterize waveguides. Preliminary results show that the refractive index change is on the order of 10^{-3}. Information about the value of refractive index change is important for design the devices. Extensions of coherence domain diagnostic techniques such as OCT can permit a direct measurement of waveguide characteristics such as scattering loss, dispersion, and wavelength dependent coupling.

Fabrication of coupled mode devices: Coupled devices are essential for functions such as photonic switching, wavelength division multiplexing, and time division multiplexing. We have recently demonstrated the fabrication of a simple multimoded X coupler. Figure 10.4 shows a microscopic image of the side and top view of the X coupler. Two waveguides are crossing at a given angle and interaction region inside the glass. When a 544 nm He-Ne laser beam was introduced into one of the two input ports, two output beams were observed, which demonstrates coupling between two branches. This current device is multimoded, however with improved exposure control, single mode couplers should be achieved.
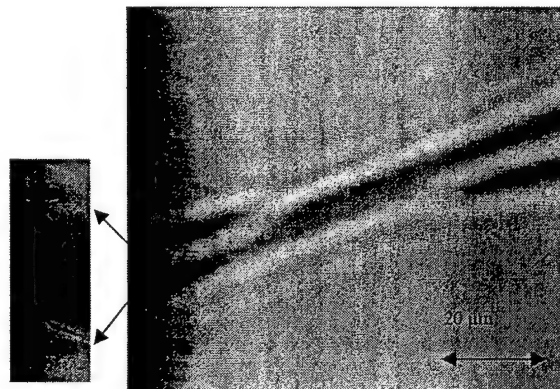

Figure 10.4: Microscopic image of the side and top view of an X coupler. 12.5 mm long, 1.1 degree crossing angle.

References for Section 10

1. K.M. Davis, K. Miura, N. Sugimoto, and K. Hirao, "Writing waveguides in glass with a femtosecond laser," Opt. Lett. 21, 1729 (1996).
2. D. Homoelle, S. Wielandy, A.L. Gaeta, N.F. Borrelli, and C. Smith, "Infrared photosensitivity in silica glasses exposed to femtosecond laser pulses," Opt. Lett. 24, 1311 (1999).
3. P. Bado, "Ultrafast pulses create waveguides and microchannels," Laser Focus World, April, 73 (2000).
4. C.B. Shaeffer, A. Brodeur, and E. Mazur, "Femtosecond laser micromachining of bulk glass at oscillator energies," in OSA Annual Meeting 1999, paper WLL160.
5. Y. Sikorski, A.A. Said, P. Bado, R. Maynard, C. Florea, and K.A. Winick, "Optical waveguide amplifier in Nd-doped glass written with near-IR femtosecond laser pulses," Elect. Lett. 36, 226 (2000).

Publications acknowledging AFOSR support under Contract No. F49620-98-1-0139

1. H. A. Haus, I. Sorokin and E. Sorokin, "Raman-induced Redshift of Ultrashort Modelocked Laser Pulses," Opt. Lett. 15, 223-231, January 1998

2. D.J. Jones, K.L. Hall, H.A. Haus and E.P. Ippen, "Asynchronous Phase-Modulated Optical Fiber-Ring Buffer", Optics Lett. 23, pp. 177-179, 1998.

3. D.J. Jones, H.A. Haus, L.E. Nelson and E.P. Ippen, "Stretched-Pulse Generation and Propagation", IEICE Trans. Electron. E81-C, pp. 180-188, 1998.

4. D.J. Jones, S. Namiki, D. Barbier, E.P. Ippen and H.A. Haus, "116-fs Soliton Source Based on an Er-Yb Codoped Waveguide Amplifier", IEEE Photon. Technol. Lett. 10, May 1998.

5. C.X. Yu, M. Margalit, E.P. Ippen and H.A. Haus, "Direct Measurement of Self-phase Shift due to Fiber Nonlinearity," Opt. Lett. 23, pp. 679-681, May 1998.

6. Y. Chen and H. A. Haus, "Dispersion-managed Solitons with a Net Positive Dispersion," Opt. Lett. 23, 1013-1015, July 1998.

7. H.A. Haus, "The Noise Figure of Optical Amplifiers," IEEE Photon Technol. Lett. 10, 1602-1604, November 1998.

8. D.J. Jones, Y. Chen, H.A. Haus and E. P. Ippen, "Resonant Sideband generation in stretched-pulse fiber lasers," Opt. Lett. 23, pp. 1535-1537, October, 1998.

9. W.S. Wong, P. B. Hansen, T. N. Nielson, M. Margalit, S. Namiki, H. A. Haus and E.P. Ippen, "In-band Amplified Spontaneous Emission Noise Filtering with a Dispersion-Imbalanced Nonlinear Loop Mirror, J. Lightwave Tech. 10, pp. 1768-1772, October, 1998.

10. E.R. Thoen, G. Steinmeyer, P. Langlois, E. P. Ippen, G. E. Tudury, C. H. Brito-Cruz, L. G. Barbosa and C. L. Cesar, "Coherent Acoustic Phonons in PbTe Quantum Dots", Appl. Phys. Lett. 73, pp. 2149-2151, October, 1998.

11. I.P. Bilinsky, J.G. Fujimoto, J.N. Walpole and L.J. Missaggia, "Semiconductor-Doped-Silica Saturable-Absorber Films for Solid-State Laser Mode Locking ", Opt. Lett. 23, pp. 1766-1768, November, 1998.

12. E.P. Ippen, D.J. Jones, L.E. Nelson and H.A. Haus, "Ultrafast Fiber Lasers," Ultrafast Phenomena XI, Chem. Phys. Vol. 63, pp. 30-34, Springer Verlag, November, 1998.

13. K.L. Hall, E.R. Thoen and E.P. Ippen,, "Nonlinearities in Active Media", *Semiconductors and Semimetals*, Chapter 2, Vol 59, Eds. E. Garmire and A. Kost, Academic Press, November, 1998.

14. W. S. Wong, H. A. Haus, L. A. Jiang, P. B. Hansen, and M. Margalit, "Photon statistics of amplified spontaneous emission noise in a 10-Gbit/s optically preamplified direct-detection receiver," Opt. Lett. 23, 1832-1834, December 1998.

15. Y. Chen and H. A. Haus, "Dispersion-managed solitons in the net positive dispersion regime," JOSA B 16, 24-30, January 1999.

16. E.P. Ippen, D.J. Jones, W.S. Wong, L.E. Nelson and H.A. Haus, "Fiber Devices for Ultrahigh-Speed Photonics," Trends in Optics and Photonics, Vol. 23, H.A. Haus, ed., Optical Society of America, January, 1999.

17. U. Morgner, F.X. Kärtner, S.H. Cho, Y. Chen, H.A. Haus, J.G. Fujimoto, E.P. Ippen, V. Scheuer, G. Angelow and T. Tshudi, "Sub-Two-Cycle Pulses from a Kerr-Lens Mode-Locked Ti:sapphire Laser", Opt. Lett. 24, pp. 411-413, March, 199S.

18. H. Cho B.E. Bouma, E.P. Ippen and J.G. Fujimoto, "Low-repetition-rate high-peak-power Kerr-Lens Mode-Locked Ti:Al$_2$O$_3$ Laser with a Multiple-pass Cavity", Opt. Lett. 24, pp. 417-419, March, 1999.

19. I.P. Bilinsky, R.P. Prasankumar and J.G. Fujimoto, "Self-Starting Mode Locking and Kerr-Lens Mode Locking of a Ti:Al$_2$O$_3$ Laser by Use of Semiconductor-Doped Glass Structures", J. Opt. Soc. Am. B., 16, pp. 546-549, April, 1999.

20. I.P. Bilinsky, J.G. Fujimoto, J.N. Walpole and LJ. Missaggia, "InAs-Doped Silica Films for Saturable Absorber Applications", Appl. Phys. Lett. 74, pp. 2411-2413, April, 1999.

21. E.R. Thoen, E.M. Koontz, M. Joschko, P. Langlois, T.R. Schibli, F.X. Kärtner, E.P. Ippen and L.A. Kolodziejski, "Two-photon Absorption in Semiconductor Saturable Absorber Mirrors", Appl. Phys. Lett. 74, pp. 3927-3929, June, 1999.

22. S.H. Cho, B.E. Bouma, E.P. Ippen and J.G. Fujimoto, "Low-Repetition-Rate High-Peak-Power Kerr-Lens Mode-Locked TiAl$_2$O$_3$ Laser with a Multiple-Pass Cavity," Optics Lett. 6, pp. 417-419, 1999.

23. U. Morgner, F.X. Kärtner, S.H. Cho, Y. Chen, H.A. Haus, J.G. Fujimoto, E.P. Ippen, V. Scheuer, G. Angelow and T. Tshudi, "Sub-Two-Cycle Pulses from a Kerr-Lens Mode-Locked Ti:sapphire Laser," Optics Lett. 24, pp. 411-413, 1999.

24. E.R. Thoen, E.M. Koontz, M. Joschko, P. Langlois, T.R. Schibli, F.X. Kärtner, E.P. Ippen and L.A. Kolodziejski, "Two-photon Absorption in Semiconductor Saturable Absorber Mirrors," Appl. Phys. Lett. 74, pp. 3927-3929, 1999.

25. W. Drexler, U. Morgner, F.X. Kärtner , C. Pitris, S.A. Boppart, X.D. Li, E.P. Ippen and J.G. Fujimoto, "In Vivo Ultrahigh-Resolution Optical Coherence Tomography," Optics Lett. 24, pp. 1221-1223, 1999.

26. Y. Chen, F.X. Kärtner, U. Morgner, S.H. Cho, H.A. Haus, E.P. Ippen and J.G. Fujimoto, "Dispersion-Managed Mode Locking," J. Opt. Soc. Am. B., 16, pp. 1999-2003, 1999.

27. P. Langlois and E.P. Ippen, "Measurement of Pulse Asymmetry by Three-Photon-Absorption Autocorrelation in a GaAsP Photodiode," Optics Letters, 24, pp. 1868-1870, 1999.

28. P. Langlois, M. Joschko, E.R. Thoen, E.M. Koontz, F.X. Kärtner, E.P. Ippen and L.A. Kolodziejski, "High Fluence Ultrafast Dynamics of Semiconductor Saturable Absorber Mirrors, " Appl. Phys. Lett. 75, pp. 3841-3843, 1999.

29. E.R. Thoen, E.M. Koontz, D.J. Jones, D. Barbier, F.X. Kärtner, E.P. Ippen and L.A. Kolodziejski, "Erbium-Ytterbium Waveguide Laser Mode-Locked with a Semiconductor Saturable Absorber Mirror," IEEE Photonic. Tech. Lett., 12, pp. 149-151, 2000.

30. M. Joschko, P. Langlois, E.R. Thoen, E.M. Koontz, E.P. Ippen and L.A. Koldoziejski, "Ultrafast Hot-Carrier Dynamics in Semiconductor Saturable Absorber Mirrors, " Appl. Phys. Lett., 71, pp. 1383-1385, 2000.

31. E.R. Thoen, J.P. Donnelly, S.H. Groves, K.L. Hall and E.P. Ippen, "Proton Bombardment for Enhanced Four-Wave Mixing in InGaAsP-InP Waveguides, " IEEE Photonic. Tech. Lett. 12, pp. 311-313, 2000.

Conference Presentations

1. H. A. Haus and Y. Chen, "Dispersion managed stretched pulse propagation," 24th European Conference on Optical Communication, ECOC'98, Madrid, Spain, September 20-24, 1998.

2. H. A. Haus, "The Gordon-Haus effect and its control," 1998 OSA Annual Meeting (invited paper), Baltimore, MD, paper FG3, October 4-9, 1998.

3. W. Drexler, U. Morgner, C. Pitris, S. Boppart, F.X. Kärtner, X. Li, S.H. Cho, E.P. Ippen, M.E. Brezinski and J.G. Fujimoto, "Subcellular Optical Coherence

Tomography with a Kerr Lens Mode-Locked Ti:Al$_2$O$_3$ Laser," SPIE BIOS 99, Jan. 22, 1999.

4. T. Schibli, E.R. Thoen, E.M. Koontz, F.X. Kärtner, E.P. Ippen and L.A. Kolodziejki, "Suppression of Modelocked q-switching and Multiple Pulse Break-up by Two-Photon Absorption", Proc. Ultrafast Optics '99, OSA, April 1999.

5. E.R. Thoen, E.M. Koontz, D.J. Jones, P. Langlois, F.X. Kärtner, E.P. Ippen, L.A. Kolodziejski, and D Barbier, "Picosecond Pulses from an Er/Yb Waveguide Laser Passively Mode-Locked with a Semiconductor Saturable Absorber Mirror", Proc. CLEO '99, CWA3, OSA May, 1999.

6. H. A. Haus, "The master equations of mode-locking," Conference on Lasers and Electro-Optics (invited paper), CLEO'99, Baltimore, MD, paper CtuA1, May 23-28, 1999.

7. E.R. Thoen, E.M. Koontz, D.J. Jones, F.X. Kärtner, E.P. Ippen, L.A. Kolodziejski, and D. Barbier, "Suppression of Instabilities and Pulsewidth Limitation by Two-Photon Absorption in Mode-Locked Lasers", Proc. CLEO '99, CThL1, OSA, May 1999.

8. P. Langlois and E.P. Ippen, "Three-Photon-Absorption Autocorrelation in a GaAsP Photodiode", Proc. CLEO '99, CFG5, OSA, May 1999.

9. L.A. Jiang and E.P. Ippen, "Wavelength and Intensity Sampling of Optical Signals using Semiconductor Optical Amplifiers", Proc. CLEO '99, CThL6, OSA May 1999.

10. M.E. Grein, L.A. Jiang, H.A. Haus and E.P. Ippen, "A Study of Timing Restoration Dynamics in an Actively Modelocked Soliton Laser", Proc. CLEO '99, TuJ1, OSA, May 1999.

11. S.H. Cho, U. Morgner, F.X. Kärtner, E.P. Ippen, J.G. Fujimoto, J.E. Cunningham and W.H. Knox, "A 7.2 MHz High Power KLM Ti:Al$_2$O$_3$ Laser Using a Multiple Pass Long Cavity and Saturable Bragg Reflector", Proc. CLEO '99, CThR4, OSA, May 1999.

12. F.X. Kärtner, U. Morgner, S.H. Cho, Y. Chen, H.A. Haus, J.G. Fujimoto, E.P. Ippen, V. Scheuer, M. Tilsch and T. Tschudi, "Ultrashort Pulse Generation with the Ti:sapphire Laser", Proc. CLEO '99, CTuF1, OSA, May 1999.

13. P. Bilinski, R. P. Prasankumar, J. N. Walpole, L. J. Missaggia and J. G. Fujimoto, "Saturable absorber modelocking using non-epitaxially grown semiconductor-doped films," CLEO'99, Baltimore, MD, paper, CThL3, May 1999.

14. S. H. Cho, U. Morgner, F. X. Kaertner, E. P. Ippen, J. G. Fujimoto, J. E. Cunningham and W. H. Knox, "A 7.2 MHz high power KLM Ti:Al$_2$O$_3$ laser using a multiple pass

cavity and a saturable Bragg reflector," CLEO'99, Baltimore, MD, paper CThL3, May 1999.

15. J. P. Laine, B. E. Little, D. Lim, and H. A. Haus, "Novel techniques for whispering-gallery-mode excitation in silica microspheres," Integrated Photonics Research, Santa Barbara, CA, paper RtuH4, July 19-21, 1999.

16. E.P. Ippen, "Fiber Devices Ultrahigh-Speed Photonics, " Integrated Photonics Research, Santa Barbara, CA, paper RMA1 (Plenary), July 19-21, 1999.

17. M. Joschko, P. Langlois, E.R. Thoen, E.M. Koontz, E.P. Ippen, and L.A. Kolodziejski, "High Fluence Ultrafast Dynamics of Hot Carriers in Semiconductors Saturable Absorber Mirrors, " QELS 2000, San Francisco, CA, paper QFF3, May 7-12, 2000.

18. U. Morgner, F.X. Kärtner, T.R. Schibli, P. Wagenblast, J.G. Fujimoto, E.P. Ippen, V. Scheuer, G. Angelow, T. Schudi, M.J. Lederer, A. Boiko, and B. Luther-Davies, "Ultrabroadband Double-Chirped Mirror Pairs Covering One Octave of Bandwidth, " QELS 2000, San Francisco, CA, paper CthE5, May 7-12, 2000.

19. M.E. Grein, E.R. Thoen, E.M. Koontz, H.A. Haus, L.A. Kolodziejski, and E.P. Ippen, "Stabilization of an Active Harmonically Mode-Locked Fiber Laser Using Two-Photon Absorption," QELS 2000, San Francisco, CA, paper CME5, May 7-12, 2000.

20. C.X. Yu, W.S. Wong, H.A. Haus, E.P. Ippen, and A. Sysoliatin, "A GH_z Regeneratively Synchronized Passively Mode-Locked Fiber Laser for Spectrum Generation in the 1.5-µm Region," QELS 2000, San Francisco, CA, paper CMP6, May 7-12, 2000.

21. H.A. Haus, "Solitons and Polarization Mode Dispersion," QELS 2000, San Francisco, CA, paper CWE1, May 7-12, 2000.

Honors and Awards

James G. Fujimoto

Fellow, Institute of Electrical and Electronic Engineers
Fellow, Optical Society of America
Discover Magazine Award for Technological Innovation (1999)

Hermann A. Haus

Member, National Academy of Sciences
Member, National Academy of Engineering
Fellow, American Academy of Arts and Sciences

Fellow, American Physical Society
Fellow, Institute of Electrical and Electronic Engineers
Fellow, Optical Society of America
IEEE Education Medal, 1991
Frederic Ives Medal of the Optical Society of America, 1994
President's National Science Medal, 1995
Honorary doctorates: Union College, Technical University of Vienna, Universiteit Gent

Erich P. Ippen

Member, National Academy of Sciences
Member, National Academy of Engineering
Fellow, American Academy of Arts and Sciences
Fellow, Institute of Electrical and Electronic Engineers
Fellow, Optical Society of America
Fellow, American Physical Society
Quantum Electronics Award, IEEE/LEOS, 1997
Berkeley Distinguished Engineering Alumnus, 2000